Asymmetric robustness in the feedback control of the retinoic acid network response to environmental disturbances

Madhur Parihar[1,$], Liat Bendelac-Kapon[2,$], Michal Gur[2,$], Abha Belorkar[1], Sirisha Achanta[1], Keren Kinberg[2], Rajanikanth Vadigepalli[1,*], Abraham Fainsod[2,*]

[1]Daniel Baugh Institute for Functional Genomics/Computational Biology, Department of Pathology, Anatomy, and Cell Biology, Sidney Kimmel Medical College, Thomas Jefferson University, Philadelphia, Pennsylvania, 19107 USA

[2]Department of Developmental Biology and Cancer Research, Institute for Medical Research Israel-Canada, Faculty of Medicine, Hebrew University, Jerusalem 9112102, Israel

[$]equal contribution

*Corresponding authors: Rajanikanth.Vadigepalli@jefferson.edu

Abraham.Fainsod@mail.huji.ac.il

Review Codes for online datasets GEO SuperSeries GSE154408: cryfqygubnszryt

https://www.ncbi.nlm.nih.gov/geo/query/acc.cgi?acc=GSE154408

SUMMARY

Retinoic acid (RA) is a developmental signal whose perturbation is teratogenic. We show that early embryos exhibit effective RA signaling robustness to physiological, non-teratogenic, disturbances of this pathway. Transcriptomic analysis of transient physiological RA manipulations during embryogenesis supported the robustness of RA signaling by identifying mainly changes consistent with the progression of embryogenesis and not dramatic treatment-induced changes. Transcriptomic pattern comparisons revealed that RA manipulation led to a network-wide feedback regulation aimed at achieving signaling robustness and normalizing RA levels. A trajectory analysis of target gene and RA network responses identified an asymmetric robustness with a high sensitivity to reduced RA levels, and an activation threshold to increased levels. Furthemore, high robustness to increased RA inversely correlated with a low response to reduced RA. Biological replicates with similar robustness levels mounted responses whose composition likely varies based on genetic polymorphisms to achieve similar outcomes providing insights on the robustness mechanisms.

KEYWORDS

Embryo development; Retinoic acid; Xenopus embryo; time-series transcriptomics; temporal gene expression pattern analysis; developmental trajectory analysis; autoregulatory feedback control.

INTRODUCTION

Retinoic acid (RA) is one of the central regulatory signaling pathways active during vertebrate embryogenesis as well as in adult tissue homeostasis regulating the transcription of numerous downstream target genes (Campo-Paysaa et al., 2008; Clagett-Dame and DeLuca, 2002; le Maire and Bourguet, 2014; Marill et al., 2003; Mark et al., 2009; Metzler and Sandell, 2016). RA is synthesized from vitamin A (retinol) or other retinoids or carotenoids obtained from the diet (Ghyselinck and Duester, 2019; Kedishvili, 2016). During embryogenesis, changes in RA levels, signal timing or signal localization, result in severe developmental malformations arising from both abnormally low and increased RA signaling. Excessive RA signaling induces developmental malformations including brain defects, organ malformations and additional anatomical anomalies (Clagett-Dame and Knutson, 2011; Collins and Mao, 1999; Cunningham and Duester, 2015; Marill et al., 2003; Mark et al., 2009; Shenefelt, 1972). Syndromes linked to reduced RA signaling include vitamin A deficiency syndrome (VAD), DiGeorge/VeloCardioFacial syndrome (DG/VCF), Fetal Alcohol Spectrum Disorder (FASD), Congenital Heart Disease (CHD), neural tube defects, and multiple types of cancer (Coberly et al., 1996; El Kares et al., 2010; Hartomo et al., 2015; Kim et al., 2005; Kot-Leibovich and Fainsod, 2009; Pangilinan et al., 2014; See et al., 2008; Timoneda et al., 2018; Urbizu et al., 2013). RA levels are tightly regulated at multiple levels throughout life to prevent aberrant gene expression as a result of diet and other environmental changes. Discrete regulatory roles of RA are usually separated temporally and spatially, taking place in different tissues, embryonic regions, or cell types, requiring the fine-tuned regulation of the source, the level, and the gene-regulatory response to this signal. This quantitative, spatial and temporal regulation relies in part on the regulated expression and activity of RA biosynthetic and metabolizing enzymes(Dobbs-McAuliffe et al., 2004; Duester et al., 2003; Hollemann et al., 1998; Sakai et al., 2001).

RA biosynthesis involves two sequential oxidation steps: first, mainly alcohol dehydrogenases (ADH) or short-chain dehydrogenase/reductases (SDR) oxidize vitamin A (retinol, ROL) to retinaldehyde (RAL), followed by the retinaldehyde dehydrogenase (RALDH) catalyzed oxidation of RAL to RA (Duester, 2008; Kedishvili, 2016; Parés et al., 2008). RA availability is further affected by ROL, RAL, and RA binding proteins (Kono and Arai, 2015; Napoli, 2017, 2016; Schroeder et al., 2008). ROL and RAL can also be produced from retinyl ester stores or from ß-carotene from food sources (Blaner, 2019; O'Byrne and Blaner, 2013). In vertebrate gastrula embryos, RA signaling is triggered by the activation of *raldh2* (*aldh1a2*) transcription whose protein product completes the last enzymatic step in RA biosynthesis (Begemann et al., 2001; Chen et al., 2001; Grandel et al., 2002; Niederreither et al., 1999). Then, RALDH2 expression and availability is the earliest rate-limiting step in RA biosynthesis. During RA biosynthesis, substrate availability for the RALDH enzymes, RAL, is controlled by members of the SDR, ADH and AKR families (Adams et al., 2014; Billings et al., 2013; Feng et al., 2010; Porté et al., 2013; Shabtai et al., 2016; Shabtai and Fainsod, 2018). Importantly, expression of many of the enzymes involved in RA biosynthesis is spatially regulated, resulting in a gradient of RA activity peaking in the caudal end of the embryo (Dubey et al., 2018; Niederreither et al., 1997; Schilling et al., 2016). Additional spatial and temporal regulation of this signaling pathway is provided by regulated expression of other components, including retinoic acid receptors (RAR and RXR) and retinoid-binding proteins (Cui et al., 2003; Janesick et al., 2015; Lohnes et al., 1995; Mendelsohn et al., 1994; Xavier-Neto et al., 2015). Besides the maternal nutritional status that can affect the levels of RA signaling in the developing embryo, environmental exposure to chemicals such as alcoholic beverages (ethanol) or other chemicals can affect the biosynthesis of RA or the status of this signaling pathway (Paganelli et al., 2010; Shabtai et al., 2018). These observations point to the close interaction of RA signaling and the environment and the necessity to adapt the RA signaling

network to nutritional changes and insults (e.g., ethanol). This adaptation and maintenance of normal signaling levels under changing conditions is termed robustness (Eldar et al., 2004; Nijhout et al., 2019). Taken together, RA metabolic and gene-regulatory components are under feedback regulation by RA signaling which may provide robustness to the RA signal homeostasis.

A deeper understanding of the RA signaling pathway during embryogenesis is required to elucidate its multiple regulatory roles, and its regulation of the signaling robustness in the presence of environmental disturbances. Very commonly, the RA pathway is studied by increasing the levels of this signal from exogenous sources (Durston et al., 1989; Kessel, 1992; Sive et al., 1990). Alternatively, loss-of-function studies take advantage of RAR inhibitors, inverse agonists, inhibitors of RA biosynthesis, or degradation of the signal (Hollemann et al., 1998; Janesick et al., 2014, 2013; Kot-Leibovich and Fainsod, 2009). In multiple RA loss-of-function studies, the developmental malformations observed are milder than expected suggesting the presence of a compensatory mechanism conferring robustness to perturbations in RA signal (Blumberg et al., 1997; Hollemann et al., 1998; Janesick et al., 2014; Koide et al., 2001; Shabtai et al., 2018; Sharpe and Goldstone, 1997). Paradoxical teratogenic outcomes were observed in a number of RA manipulation studies, suggesting the activity of regulatory feedback mechanisms (D'Aniello et al., 2013; D'Aniello and Waxman, 2015; Lee et al., 2012; Rydeen et al., 2015). To further characterize the robustness of RA signaling during early embryogenesis we employed clearly defined and transient RA manipulations that were terminated during early gastrula, and the kinetics of recovery of the embryos was monitored by RNAseq, qPCR and phenotypic analysis for several hours thereafter. These results demonstrated a high robustness to physiological perturbations of the RA signal with relatively small transcriptome-wide changes. Further transcriptomic analysis showed that components of the RA metabolic and signaling network exhibited expression changes in a manner that is

dependent on the direction of RA manipulation, suggesting a mechanistic explanation for the robustness observed. Multiple embryo clutches, i.e. biological repeats, were analyzed. Comparative analysis of the biological repeats revealed differences between clutches in their individual robustness response to enhanced or suppressed RA signaling. These results exposed potential consequences of the underlying genetic differences between clutches as each one originated from a single female, and most *Xenopus laevis* stocks in laboratories are outbred. Our results suggest an asymmetric capacity for robust control of RA signal in the early embryo, likely contributing to the human developmental defects that arise due to imbalance, most often, a reduction) in Vitamin A levels during early development.

RESULTS

Physiological RA manipulation uncovers signaling robustness

To understand the regulatory role of RA signaling in early embryos, we routinely employ two approaches to reduce the levels of this ligand (Fig. 1A). We either partially inhibit the oxidation of retinaldehyde to RA with pharmacological RALDH inhibitors like 4-diethylaminobenzaldehyde (DEAB) (Kot-Leibovich and Fainsod, 2009; Shabtai et al., 2016; Shabtai and Fainsod, 2018), or we overexpress the RA hydroxylase, CYP26A1 (Hollemann et al., 1998; Yelin et al., 2005), that renders this signal biologically inactive (Dobbs-McAuliffe et al., 2004; Niederreither et al., 2002). Over a wide range of concentrations these treatments result in clear, but unexpectedly mild, developmental defects for such a central regulatory signaling pathway (compare Fig. 1B with Fig. 1C, D). An efficient approach to induce severe phenotypes by RA signaling loss-of-function (LOF) is to combine knock-down treatments that target the retinoid metabolism at different steps (Fig. 1A, E). These observations demonstrate

that RA metabolism and signaling exhibit strong robustness in the context of experimental manipulation of RA levels.

To study the physiological robustness of retinoic acid signaling we focused on moderate perturbations of this pathway within the range determined in *X. laevis* early embryos (about 100-150 nM all-*trans* RA) (Durston et al., 1989; Kraft et al., 1995; Kraft and Juchau, 1992; Sive et al., 1990). To empirically determine the RA concentrations to use, we tested the effects on gene expression of concentrations (1 nM - 1 μM) spanning the physiological range and above (Fig. 2). Quantitative real-time PCR (qPCR) was performed on RNA samples of treated embryos collected during early (st. 10.25) and late gastrula (st.12) (Nieuwkoop and Faber, 1967). We analyzed genes encoding enzymes involved in RA metabolism and known RA target genes during early embryogenesis. Genes positively regulated by RA at both stages, *hoxb1*, *cyp26a1*, and *dhrs3* exhibited dose-dependent responses (Fig. 2A-C). The genes *raldh2* and *rdh10,* are down-regulated by most RA doses (Fig. 2D, F), while *raldh3* (*aldh1a3*) is up-regulated earlier on and is repressed later on by the treatment (Fig. 2E). Importantly, RA concentrations as low as 10 nM had a significant effect on gene expression.

To specifically study the robustness of RA signaling in early *Xenopus laevis* embryos, we established an experimental protocol where RA levels were transiently manipulated pharmacologically within a physiological range. The perturbation was terminated by several washings to remove the treatment and then the embryos were monitored post-treatment during the recovery period. Embryos were treated with RA (10 nM) for 2 hours starting from late blastula (st. 9.5) and washed during early gastrula (st. 10.25), about 2 hours after the treatment was initiated. At different time points during the post-wash recovery period, samples were collected to perform kinetic analysis of the changes in gene expression by qPCR (Fig. 3). To monitor the changes in RA signaling levels by gene expression, two well-characterized RA-regulated genes, *hoxb1* and *hoxb4,* were studied. Expression analysis of both genes showed

that at the time of treatment washing (t_0), both genes were upregulated when compared to control sibling embryos (Fig. 3A). Two hours into the recovery, both RA target genes were back to control expression levels when compared to stage-matched, untreated sibling embryos from the same clutch. To begin understanding the robustness of RA signal and the dynamic regulation of RA metabolism we studied the expression of *dhrs3*, which encodes an enzyme that preferentially reduces retinaldehyde to retinol to attenuate RA biosynthesis (Feng et al., 2010), *cyp26a1*, which targets RA for degradation, and *raldh2* that produces RA from retinaldehyde (Shabtai et al., 2016). As expected, both negative regulators of RA signaling, *dhrs3,* and *cyp26a1*, are upregulated by the increased RA at t_0 (Fig. 3B). Their return to normal expression levels is only observed in the 4-hour samples in contrast to the *hox* genes that returned to normal expression 2 hours earlier. As expected, *raldh2* exhibited at t_0 an RA-promoted downregulation (Fig. 3B). It also took over 4 hours for this gene to return to normal expression levels. These results indicate that the expression of genes encoding RA metabolic enzymes, which themselves are regulated by RA (Fig. 2), is shifted to achieve normal RA levels in the face of external perturbation to RA levels, even though these genes remain abnormally expressed for a longer period.

A complementary study was performed by inhibiting RA biosynthesis taking advantage of DEAB (Fig. 3C,D). All genes studied exhibited fluctuations during the recovery period. Also, in this case, *hoxd1* and *hoxb1*, key targets of RA signaling, reached almost normal levels at an earlier stage than the genes encoding RA metabolic components (Fig. 3C). As expected, genes encoding anabolic enzymes, e.g., *raldh2*, were upregulated, and catabolic components, e.g., *cyp26a1*, were downregulated (Fig. 3D).

The results of the kinetic analysis of the recovery from RA manipulation by qPCR provided a novel and important support and insight into the robustness of RA signaling. We observed that while RA downstream target genes reach normal expression levels relatively

quickly, expression of genes encoding RA metabolic enzymes is maintained at seemingly abnormal levels for a longer period of time, such that their combined abnormal activity levels likely result in almost normal RA signaling levels. Such expression changes suggest the hypothesis that during early development RA signaling robustness is achieved, at least in part, via feedback control of network components aimed at preventing a significant differential system-wide gene expression response and the resulting teratogenic outcomes.

Non-teratogenic RA perturbations uncover signaling robustness at the transcriptomic scale

To gain a better understanding of the robustness of RA signaling and adaptation of the metabolic network to disturbances, we performed a kinetic transcriptomic analysis. In an attempt to optimize the kinetic study, parameters such as developmental stages and time between samples were empirically tested. The experimental design involves treating embryos for 2 hours from late blastula (st. 9.5) to early gastrula (st. 10.25) and collecting samples every 1.5 hours after terminating and washing the treatment (Fig. 4A). Embryos were treated with RA (10 nM) or DEAB (50 μM). For each biological repeat, all treatments, controls, and time points were collected from a single fertilization, from the eggs (clutch) of a single female. The efficiency of the treatments and quality of the RNA samples was initially ascertained by qPCR for changes in *hox* gene expression as a readout of the RA signal levels. Only those biological repeats where both treatments exhibited the expected up-regulation (RA) or down-regulation (DEAB) in *hox* gene expression were selected for RNA-seq.

We analyzed the time series transcriptomic data set for differential expressed genes using a two-way ANOVA (t=0, 1.5, 3, 4.5 hours; treatments: RA, DEAB, control; n=6 biological replicates). Principal Component Analysis (PCA) of the gene expression variation showed that all samples separated progressively along the first principal component (PC1)

which corresponds to the developmental stage (Fig. 4B). Surprisingly, RA manipulated samples clustered with the control samples of the same developmental stage. Normal transcriptomic changes as a result of progression through embryogenesis appear to be the dominant variable distinguishing between the samples irrespective of treatment (Fig. 4B). The second component (PC2) separated the sample groups at intermediate time points (1.5 and 3h) from those at 0 and 4.5h time points, indicating a transient differential expression shift as the next most dominant pattern in the data. The effect of the RA and DEAB treatments on the transcriptome was not readily apparent in the next seven principal components. The the eighth principal component (PC8) showed some separation of DEAB group from RA and Control groups (Fig. 4C), whereas the tenth principal component (PC10) showed some separation of the RA treatment group from Control and DEAB treatments (Fig. 4D). The top-ranked genes along PC8 and PC10 showed distinct dynamic patterns across the treatments, whereas top-ranked genes along PC1 and PC2 largely corresponded to in-common dynamic changes over time (Fig. 4D; Supplemental Fig. S1). The patterns of both opposed RA manipulations, RA and DEAB, closely resembled the control sample for the top-ranked genes along PC1 and PC2, further supporting the normal developmental changes as the dominant pattern. The overall magnitude of induced changes in gene expression in response to the RA or DEAB treatments appears to be less than the normal transcriptome changes occurring during early developmental stages, showing that RA signaling robustness possibly dampens the gene expression changes otherwise induced by abnormal RA levels. Taken together, these results suggest that the RA and DEAB treatments, applied at moderate physiologically relevant concentrations, do not alter the transcriptome extensively in the whole embryo. These results are consistent with the response of a robust system that functions to limit the gene expression changes in the majority of the transcriptome.

Dynamic pattern analysis reveals the molecular genetic mechanisms underlying the RA robustness response

In order to characterize the molecular transcriptomic mechanism for the robustness response following the RA and DEAB treatments, we analyzed the clutch-averaged data using an unbiased dynamic pattern analysis approach to categorize the gene expression profiles along all possible discretized patterns (Kuttippurathu et al., 2016). Our analysis revealed a total of 4693 significantly differentially expressed genes with greater than 2-fold changes over time (compared to t=0 within each treatment group; multiple testing corrected q-value < 0.05). For each gene, a pattern based on the direction of up- or down-regulation above a 2-fold threshold (three possibilities: up-regulation, down-regulation, or no change) at each of the three recovery time points relative to early gastrula (t=0) was determined. This pattern analysis theoretically should yield 3*3*3 = 27 possible discretized patterns. Such an exhaustive approach allows us to enumerate the dominant as well as subtle patterns in the data and overcomes limitations of conventional cluster analysis that is likely to miss or mask the smaller groups of genes with distinct expression profiles over time. In our analysis, not all possible dynamic patterns had representative genes. Out of the 27 possible dynamic patterns, only 10 patterns were exhibited by genes in the transcriptome in at least one of the three experimental groups (RA, DEAB, Control) (Fig. 5A). Of these, only 5 patterns were exhibited by a substantial number of genes (>100) in at least one of the three experimental groups. These five patterns correspond to up- or down-regulation at later time points (3h and 4.5h), and persistently induced or suppressed expression at all three recovery time points, including progressive changes in gene expression over time (Fig. 5A). At the 2-fold threshold, there were no genes that showed down-regulation first and then up-regulation and vice versa. There were no significant differences in the gene counts between RA or DEAB and control groups (two-tailed Z test, $p > 0.05$). Analysis of statistically enriched pathways and processes (Gene Ontology analysis) in the control group

highlighted several functional annotations including development, cell cycle, morphogenesis, RA biosynthesis, gastrulation, and others. (Fig. 5B; Supplemental Table S1). These expression dynamics are consistent with the changes occurring in the early gastrula stage when the endogenous RA system is activated. The patterns with relatively fewer genes (<100) correspond to transient up- or down-regulation at 3h that is normalized by 4.5h, as well as progressive down-regulation.

The results shown in Fig. 5 highlight two aspects of the effect of perturbations in the RA signal. First, at the 2-fold threshold, there are no distinctive dynamic patterns of gene expression changes that occur only in response to RA or DEAB treatment conditions. Second, the number of genes per pattern is of a similar order of magnitude between the two treatments and control. These results suggest that, at physiologically relevant concentrations employed here, RA and DEAB treatments modulate the transcriptional and post-transcriptional regulators at a scale resembling the changes in controls, albeit with differences in potential targets. For instance, only a subset of genes that showed late down-regulation (first row in Fig. 5A) were common across all the three groups (772 genes, Fig. 5C). Several genes showed similar late down-regulation between the treatments or between one of the treatments and the Control group (Fig. 5C). In addition, many genes showed a late down-regulation pattern only in one of the treatment groups or in the Control (Fig. 5C). While the Venn diagram analysis (Fig. 5C) revealed extensive overlap between the RA and DEAB treatments and Control samples within a given differential regulation pattern, the overlap across patterns is not immediately clear from this analysis.

In order to exhaustively compare the RA and DEAB treatment groups for their effect on gene expression relative to the unperturbed temporal pattern observed in the control samples, we adapted a recently developed unbiased approach named COMPACT for analyzing time-series differential transcriptomic profiles across multiple experimental conditions

(Kuttippurathu et al., 2016). In this scheme, we started with the statistically significant genes within each treatment group (two-way ANOVA; $q<0.05$), and constructed discrete patterns based on differential gene expression between RA and control groups (81 theoretically possible patterns, with up-, down- and no-regulation at t=0, 1.5, 3 and 4.5 h). In parallel, we constructed similar discrete patterns for the DEAB versus control groups. Only the patterns with at least one gene in either comparison were included in the subsequent analysis, yielding 32 distinct patterns (Fig. 6A). Finally, we intersected the two distributions to create a matrix of comparative patterns where each element corresponds to a distinct pair of patterns corresponding to RA vs. control and DEAB vs. control (Fig. 6B). The discrete patterns were based on a 1.3-fold average difference between RA (or DEAB) and control groups at each of the four time points. The effect size threshold was chosen at a lower level than 2-fold as the differential expression analysis revealed that the RA/DEAB perturbations were leading to a smaller magnitude of changes at each time point, as compared to the larger changes occurring normally over time, additional suggestive evidence of robustness.

Analysis of the COMPACT matrix (Fig. 6B, Extended Data 1) demonstrates that the majority of the genes sensitive to the RA signal manipulation exhibited sensitivity to only one direction of the RA perturbation. A total of 193 genes showed a response only to the addition of exogenous RA relative to Control (middle row), whereas 224 genes were only responsive to inhibition of RA production by DEAB (middle column). Of the genes that showed responses to both RA and DEAB perturbations, 88 genes showed up-regulation or down-regulation irrespective of RA or DEAB treatment (quadrants a and d in Fig. 6B). A set of 48 genes showed opposite transcriptional outcomes in response to exogenous RA increase versus inhibition of RA production (quadrants b and c in Fig. 6B). Interestingly, the set of genes that showed up-regulation by exogenous RA addition and down-regulation by DEAB (quadrant b) contained several genes involved in the biosynthesis and metabolism of RA (Fig. 6C).

We mapped the expression changes shown in Fig. 6B to the RA signaling and metabolic network (Fig. 6D,E). Notably, genes encoding proteins involved in suppressing RA levels (*cyp26a1*, *dhrs3*) were up-regulated and the genes encoding for proteins involved in RA production (*aldh1a2*, *aldh1a3*, and *rdh10*) were down-regulated in response to transient increase in RA. These genes showed opposite regulation in response to exogenous inhibition of RAL to RA oxidation by DEAB (Fig. 6E). As an independent evaluation, we analyzed the differential expression time series data using another unbiased approach, weighted gene correlation network analysis (WGCNA) (Langfelder and Horvath, 2008). Manual examination of WGCNA indicated that one of the correlated gene expression modules (highest correlation with treatment) contained a similar gene set as shown in Fig. 6C, supporting the findings from our COMPACT analysis (green module in WGCNA results, Supplemental Table S2; Extended Data 2). Taken together, our results support a mechanism aimed at maintaining homeostasis of the RA signaling levels to counter the effects of exogenous perturbations, nutritional and environmental, and prevent teratogenic effects by a transcriptional feedback control system.

Clutch-wise heterogeneity demonstrates multiple alternative mechanisms to recover from RA perturbations

The analysis above describes RA as a robust signaling pathway capable of responding to environmental disturbances. Our results show that an important aspect of the regulation of robustness involves changes in RA network components, and identified the main RA network components responding during early gastrulation (Fig. 6). Interestingly, the PCA analysis suggested clutch-specific heterogeneity in gene expression changes where all samples from the same clutch tended to cluster together but the different clutches separated slightly from each other (Fig. 4B,C; Supplemental Fig. S2). For these reasons, we analyzed the transcriptional changes in the RA metabolic network within each clutch. We sought to determine whether the

clutch-to-clutch variation observed in the RNAseq data is evident even if we utilize a different technical approach to measure the changes in gene expression in a separate set of manipulated embryos. Hence, we generated an additional set of samples to study the dynamic expression changes in RA metabolic network genes using high-throughput real-time PCR (HT-qPCR; Fluidigm Biomark). This separate cohort of six additional clutches (biological repeats labeled G-L) treated with RA or DEAB following the same experimental design (Fig. 4A) used for RNAseq study of the original six clutches (A-F). We designed PCR primers for multiple members of the RA metabolic network and a number of *Hox* genes as targets of the RA signal (Supplemental Table S2). Our results show that the heterogeneity between clutches observed in the HT-qPCR data resembles the clutch-to-clutch variation evident in the RNAseq data (Supplemental Figs. S2 and S3).

We ordered the 12 biological repeats (clutches) according to the earliest time at which *hoxa1* returned to the baseline levels (Fig. 7). This ordering intermingled the clutches of the RNAseq and HT-qPCR analysis. Our analysis identified high variability in the response to the RA and DEAB treatments among the individual clutches. Clutches with significant up-regulation of *hoxa1* expression as a result of RA addition showed limited down-regulation in expression in response to inhibition of RA biosynthesis (DEAB treatment; clutches C, L, J, K, H, I in Fig. 7). The opposite response was also observed where DEAB induced a strong response on *hoxa1* expression while the RA treatment induced a mild to very weak response (clutches E, D, F, G, A, B in Fig. 7). Examining the clutch-to-clutch variation in the extent of changes in gene expression revealed a heterogenous correspondence between *hoxa1* and RA metabolic network genes. The suppressors of RA signaling, e.g., *cyp26a1* and *dhrs3*, showed significantly altered expression in clutches (C, L, J, K, H) with larger deviations in *hoxa1* expression and a strong and extended response to the addition of RA. In contrast, the extent of

differential expression of the RA producers (e.g., *aldh1a2* and *rdh10*) after RA manipulation was relatively mild and did not fully align with the deviation in *hoxa1* expression (Fig. 7). Such a heterogeneous correlation between extent of feedback regulation and clutch-to-clutch variation in *hoxa1* expression was observed across the RA metabolic network (Supplementary Fig. S4).

Asymmetry of robustness in response to increase versus decrease in RA signal

We sought to quantitatively rank the robustness of each clutch in an integrated manner based on the extent of shift in multiple *hox* genes and the complementary feedback regulatory response of the RA metabolic network genes. To this end, we pursued a trajectory-based approach in which the temporal evolution of RA or DEAB treatment groups were compared to their controls based on the regulatory outcome of target gene expression and RA network feedback regulatory gene expression. In this analysis, the samples of all biological repeats (clutches) at all time points were projected onto the first three principal components based on the expression of *hox* genes (*hoxa1*, *hoxa3*, *hoxb1*, *hoxb4*, *hoxd4*) or of RA metabolic network genes. A principal curve was fit to the projected data, representing the trajectory in which the system evolves over time for all clutches combined. Each clutch was visualized separately along the principal trajectory, allowing us to compare the temporal evolution of deviations (distances) between treated samples and controls (select clutches shown in Fig. 8A and 8B; all clutches included in Supplemental Fig. S5). As a multi-gene measure of robustness of each clutch, the net absolute distance between the treated samples (RA or DEAB), and controls at all time points, was computed along the principal curve in the *hox* gene or the RA network trajectory maps. Our results revealed a wide range of clutch-to-clutch variability in robustness as assessed by the integrated deviation from the control trajectory of multiple *hox* genes (Fig. 8C; Supplemental Fig. S5). The distance between the treatments and controls decreased over

time in nearly all the clutches with significant differences in the time taken to close the gap (Fig. 8C). Clutches with low robustness to RA addition showed larger distances between RA-treated samples and controls along the *hox* gene trajectory at any given time point (e.g., Fig. 8A, clutch C), compared to robust clutches with decreasing distances between RA-treated samples and controls over time (e.g., Fig. 8A, clutch E). By contrast, DEAB treatment resulted in an opposite pattern of robustness to that of RA addition (Fig. 8B). For example, clutch C showed the widest deviation from control samples in the *hox* gene trajectory, whereas clutch E showed least deviation (Fig. 8B top row and Fig. 8C). Clutch J exhibited intermediate robustness responses to both the increase and the reduction of RA levels (Fig. 8A,B). The anti-correlated pattern of robustness to increase versus decrease in RA levels suggests an asymmetric tradeoff in the early embryo in the ability to counter changes in RA levels (Fig. 8E). The *hox* responses to decreased and increased RA levels revealed that all biological repeats aligned along a diagonal and covered the whole range of responses (Fig. 8E). This result suggested the establishment of an RA gradient among the clutches.

In contrast, similar analysis of the RA network component changes showed a scattered pattern of the biological repeats with no clear trend. The feedback regulatory response based on the RA metabolic network trajectory map (Fig. 8A and 8B bottom rows; Supplemental Fig. S5) was variable across clutches, with a characteristic pattern of reduced deviation over time in several clutches (Fig. 8D). There was no significant correlation (or anti-correlation) in the net shift in feedback regulatory action between RA addition versus reduction (Fig. 8F). Interestingly, the scattering distribution depended on the direction of the RA manipulation. The range of clutch distribution along the x- axis in Fig. 8F suggests an immediate response to any reduction in RA levels, and an upper limit to this response that points to a constrained ability to mount a corrective feedback regulatory action for large reductions. In contrast, the clutch distribution along y-axis suggests that the response to increased RA requires a minimal change

to be activated and it exhibits an upper threshold (Fig. 8F). These observations suggest a high sensitivity to RA reduction but a lower sensitivity to slight RA increase.

An efficiency-efficacy matrix organizes the clutch variability in robustness and feedback regulation

We examined if the asymmetric robustness to direction of RA change in correlates to the extent of feedback regulatory action (Fig. 9). We formulated a "efficiency-efficacy matrix" (Fig. 9A). The sections of this matrix delineate distinct possibilities based on all permutations of the extent of robustness and the phenotypic outcome, i.e., the net shift in the *hox* gene trajectory, versus extent of the feedback regulatory response, i.e., the net shift in RA metabolic network trajectory. In this scheme, a high robustness (low net shift along the *hox* gene trajectory) may be achieved by a mild or a strong response in the RA metabolic network gene expression, yielding efficient and effective closed-loop feedback control scenarios, respectively (lower quadrants in Fig. 8A). Similarly, the cases of low robustness (high net shift along the *hox* gene trajectory) may be characterized by mild or strong gene expression changes in the RA metabolic network components, corresponding to inefficient or ineffective closed-loop feedback control, respectively (upper quadrants in Fig. 9A). In response to an increase in RA levels, half of the clutches were distributed within the efficient and effective zone of the robustness efficiency matrix (Fig. 9B; blue letters). Five clutches exhibited a substantial shift in *hox* and RA network expression in response to increased RA, suggesting an inability to correct the RA change, i.e. ineffective response. One clutch was located in an inefficient zone as it exhibited a substantial shift in *hox* gene expression along with a limited extent of gene expression shift in RA metabolic network components. By contrast, the distribution of clutches in response to reduction in RA levels (DEAB treatment) distributed between the efficient and inefficient quadrants, characterized by limited gene expression shift in the RA metabolic

network while yielding a wide range of robustness in *hox* gene expression (Fig. 9B; green letters).

We examined if the clutches with similar levels of robustness and overall feedback regulation use similar strategies for feedback regulation, i.e., whether they show similarity in the genes that are differentially regulated in response to RA manipulation. Interestingly, we found that the identity of differentially regulated genes in the RA metabolic network can vary between clutches co-localized in the efficiency-efficacy matrix (Figs. 6E and 9C). For example, in response to addition of RA, clutches A, E and F showed similar differential regulation of *dhrs3*, *aldh1a2,* and *cyp26a1*, but diverged in the regulation of other genes such as, *stra6*, *sdr16c5*, *adhfe1*, *rdh13*, *aldh1a3*, and *cyp26c1* (Fig. 9C). Similarly, in response to DEAB treatment, clutches A, B and D showed downregulation of *dhrs3* and *cyp26a1*, and upregulation of *rbp1*, suggesting feedback aimed at reducing activity of biochemical processes leading to reduction in RA levels, and increasing import of retinol. However, there was much variability across these clutches in the differential expression of *aldh1a2* and *aldh1a3*, i.e., the feedback control aimed at increasing the production of RA (Figs. 6E and 9D). Taken together, the results described in Figs. 8 and 9 provide strong evidence that the early embryo is differentially capable of responding to increase versus decrease in RA levels, with a distinct range of feedback regulatory responses elicited between the two scenarios.

DISCUSSION

Robustness of the retinoic acid signaling pathway

Signaling pathway robustness is a central characteristic of all regulatory networks to ensure signaling consistency and reliability. Variations in signaling levels can arise as a result of changing environmental conditions or genetic polymorphisms that can affect the expression or

activity level of network components. We describe a systems biology approach to study the robustness of RA metabolism and signaling based on transient manipulation of ligand levels. Gastrula stage *Xenopus laevis* embryos have been reported to contain RA levels, around the 100 nM - 150 nM range (Durston et al., 1989; Kraft et al., 1995; Kraft and Juchau, 1992). In contrast, due to the clear and severe developmental defects induced, *Xenopus* embryos, and many other systems, are commonly treated with RA concentrations in the 1 μM to 10 μM range to perturb this signaling pathway (Sive et al., 1990; Taira et al., 1994). To focus our robustness study of RA signaling to the physiological range, we showed that by increasing the RA levels by as little as about 10% (10 nM) we could consistently induce expression changes in RA-regulated genes. Interestingly, embryo treatments with RA concentrations in the physiological range exhibit very slight developmental malformations suggesting the induction of compensatory mechanisms to control morphogen signaling and prevent abnormal gene expression (Hollemann et al., 1998; Reijntjes et al., 2005; Sive et al., 1990). We obtained similar results when we reduced the levels of RA by either blocking the biosynthesis (DEAB treatment) or by targeting this ligand for degradation (CYP26A1 overexpression). These observations are supported by multiple loss-of-function studies describing mild developmental malformations induced by RA signaling reduction (Blumberg et al., 1997; Hollemann et al., 1998; Janesick et al., 2014; Koide et al., 2001; Kot-Leibovich and Fainsod, 2009; Shabtai et al., 2018; Sharpe and Goldstone, 1997; Shukrun et al., 2019). Therefore, increased or decreased RA levels in the physiological range result in mild developmental defects, suggesting the activation of compensatory mechanisms. We show that one approach to overcome the robustness of RA signaling is to interfere with the metabolic/signaling network at two different steps as in the case of DEAB together with CYP26A1. A possible explanation for this outcome is that manipulating the RA network at more than one point hampers its ability to efficiently elicit a feedback regulatory response.

RA signaling robustness was further analyzed taking advantage of transient RA manipulations and the temporal kinetic, transcriptome-wide (RNAseq) analysis of the restoration of normal gene expression patterns. The large expression differences observed corresponded to normal transcriptome changes resulting from the progression through embryogenesis. The close clustering of the RA-manipulated (increased or decreased RA) and control samples at each time point further supports the robustness of this signaling pathway. Alternatively, the treatments were inefficient, a possibility we could rule out by qPCR screening of all RNA samples for *Hox* expression changes prior to sequencing and subsequent computational analysis of the RNAseq data for individual gene expression shifts. Therefore, the PCA analysis suggests the activation of an efficient robustness response of the RA network to maintain normal, non-teratogenic, target gene expression levels during early gastrulation.

The RA robustness response emerges from autoregulatory changes in the RA metabolic network

Our results clearly support the robustness of RA signaling when manipulated within the physiological range. Then, how is this robustness achieved? What is the mechanism activated to achieve RA robustness? Is the RA metabolic network modified to bring about this robustness? The qPCR analysis already provided insights on the RA robustness mechanism. RA target genes affected by the treatment revealed abnormal expression levels at the end of the manipulation (t=0), and for some target genes (*hox*), we observed a speedy return to normal expression levels already after 1.5 hours from the end of the treatment. Genes encoding components of the RA metabolic network also exhibited abnormal expression levels at t=0. Interestingly, their return to normal transcript levels was delayed beyond the time required for the RA targets to reach normal expression. These observations suggest a scenario where the RA metabolic network through an RA-dependent feedback regulatory mechanism is altered in

an attempt to restore normal signaling and target gene expression levels. Multiple reports have described the regulation of select individual RA network component expression by RA. Most of these studies deal with RA treatments resulting in the up-regulation of enzymes involved in the suppression or reduction of RA signaling like CYP26A1, ADHFe1, and DHRS3, and down-regulation of RA producers (anabolic enzymes) like RALDH2 and RDH10 (Chen et al., 2001; Dobbs-McAuliffe et al., 2004; Fujii et al., 1997; Hollemann et al., 1998; Kam et al., 2013; Sandell et al., 2012; Shabtai et al., 2017; Sonneveld et al., 1998; Strate et al., 2009).

To understand the full extent of kinetic response to transient RA manipulation, we pursued a transcriptome-wide analysis of the recovery kinetics. Out of the 27 possible kinetic patterns consisting of upregulation, downregulation or no change following treatment and washing, only 10 were represented in any of the treatment or control samples, and only five patterns were exhibited by a substantial number of genes (n>100). These observations suggest that among the RA-regulated genes, direct or indirect, there is a limited number of possible regulatory outcomes either in an attempt to normalize RA levels, i.e. robustness, or as target genes. Although this classification is qualitative and there might be differences in intensity, it suggests a limited repertoire of RA regulatory responses. To further understand the regulation of RA targets we performed a comparative analysis of the patterns observed during increased and decreased RA levels using our unbiased approach, COMPACT (Kuttippurathu et al., 2016). This analysis revealed that most genes (75.40%) responding to RA manipulation and recovery exhibited a response to either increased or decreased RA levels. Only 48 genes out of 553 (8.67%) exhibited reciprocal responses to both, increased and decreased RA levels. Interestingly, many of these genes are involved in RA metabolism or signaling, in agreement with their function in maintaining non-teratogenic RA levels.

Our results provide an integrative network-wide view that incorporates the concerted feedback regulation of multiple pathway components to achieve normal signaling under

changing environmental conditions. The temporal discrepancy in the return to normalcy between targets and network components and the network-wide changes in expression patterns suggests a response taking place at multiple levels. The initial response to changes in RA levels will most probably be mediated by the actual enzymes and factors already present in the cell. In parallel, the same change in RA signaling will initiate a transcriptional response which in the case of increased RA will involve not only the up-regulation and eventual enhancement of the enzymatic RA suppressor activity, i.e. DHRS3, ADHFe1, and CYP26A1, but importantly, a complementary down-regulation and activity reduction in RA producing enzymes (RALDH2 and RDH10). This transcriptional response will necessarily exhibit a slight delay until fully functional as the network component genes will have to undergo transcription, followed by translation and post-translational modifications, when required.

We observed that the expression of some RA network components exhibits oscillatory behavior close to control expression levels, probably as a result of the fine-tuning of the RA signal. This fine-tuning of the RA signal levels coupled to the inherent delay in the transcriptional response could transiently result in the inversion of the overall signaling direction, and an oscillatory transcriptional behavior. In a few instances such paradoxical observations of RA signaling outcome following RA manipulation, i.e. overcompensation, have been reported (D'Aniello et al., 2013; Lee et al., 2012; Rydeen et al., 2015). These observations identify a very dynamic feedback regulatory network continuously fine-tuning itself in response to perturbations.

Asymmetric response to increased and decreased RA levels

Our study provided new insights on the network responses to increased and decreased RA levels. One important outcome from our study is the observation that the responses to increased and decreased RA are not inverse but rather governed by different regulatory rules. These observations were reached by performing a trajectory-based analysis in an attempt to rank the

RA robustness based on the response of *hox* genes as RA targets, and the extent of transcriptomic changes of the components of the RA network. We derive the following primary conclusions regarding this asymmetry of RA signal robustness:

First, the response to reduced RA signaling is activated after very slight reduction, while the response to increased RA is only activated above a threshold. Also, the response to reduced RA reaches a lower upper threshold than the response to increased RA. The alignment of the *hox* responses along a diagonal suggested the establishment of an RA gradient among the clutches. In contrast, the network responses showed no clear trend across clutches. Notably, the network responses show different thresholds depending on the direction of the RA manipulation. These observations suggest a high sensitivity to RA reduction but a lower sensitivity to slight RA increase, i.e., an asymmetric capacity to mount responses dependent on the direction of RA changes.

Second, very efficient responses to reduced RA are accompanied by weak responses to increased RA, within the same clutch. The inverse situation was also observed suggesting an asymmetric response to RA manipulations. The alignment of the robustness responses, *hox* changes, fitted a diagonal with a negative slope. This negative slope suggested that while a clutch might very efficiently deal with increased RA, i.e. high robustness, the same clutch struggles to compensate for a reduction in RA, i.e. low robustness. The inverse situation, and also more "balanced" clutches were observed. These observations suggest that not only sensitivity response thresholds are involved, but also the robustness capacity to increased and decreased RA are interconnected in an inverse fashion. These observations led us to formulate an efficiency-efficacy matrix to link the robustness response of the RA network to the outcome of their activity as detected by the *hox* response.

Third, different clutches with similar robustness levels to increased or reduced RA levels can mount robustness responses by incorporating different components of the RA network. The

transcriptomic and HT-qPCR analyses allowed us to perform a detailed determination of the network components comprising the robustness response, i.e. the mechanism of the robustness. Clutches in proximity in the trajectory-based analysis or in the efficiency-efficacy matrix mount responses by changing different sets of genes. The RA network includes multiple components, i.e. enzymes, whose biochemical activity overlaps or is very similar. The RA producing genes, *aldh1a1, aldh1a2,* and *aldh1a3*, also known as *raldh1, raldh2,* and *raldh3* respectively are one example. All three enzymes oxidize retinaldehyde to produce RA (Cunningham and Duester, 2015; Kedishvili, 2016, 2013; Shabtai et al., 2016). Some of the differences between them apparently include enzymatic efficiencies and their expression patterns including location, timing, and intensity (Blentic et al., 2003; Chen et al., 2001; Lupo et al., 2005; Romand et al., 2004; Shabtai et al., 2018). A similar situation can be argued for enzymes with RA degrading or biosynthetic suppressing activity like CYP26A1, B1, and C1, or DHRS3, ADHFe1, RDH13 and others (Belyaeva et al., 2017, 2008; Hollemann et al., 1998; Shabtai et al., 2017; Sonneveld et al., 1998). Some of these enzymes can reduce or prevent the production of retinaldehyde while others make the RA biologically inactive targeting it for degradation. Irrespective of the biochemical mechanism, these enzymes function to prevent excessive RA signaling. These observations suggest that in the RA network where redundant enzymes and factors performing similar activities are common, a robustness response can be established using different components to reach the same level of robustness.

Fourth, genetic polymorphisms probably explain in part the different responses between clutches to increased or decreased RA levels, and the metabolic and regulatory composition of such responses. In our experiments, we utilized commercially available *Xenopus laevis* laboratory stocks which are outbred and exhibit extensive genetic variability (Savova et al., 2017). Therefore, we propose that one of the main differences between clutches in their response to RA manipulation is probably the result of genetic variability. Formally, technical

issues could somehow account for some of the clutch-to-clutch variability uncovered in the PCA analysis. To further support the genetic basis of the RA response, we analyzed six additional clutchesby high-throughput real-time PCR. This qPCR analysis showed that the new clutches exhibit overlapping responses to RA manipulation to the clutches analyzed by RNAseq. These observations further supported the involvement of genetic variability. We mined the Savova et al. (2017) data identifying multiple polymorphisms in RA network components (Supplemental Table S4). All these observations support the potential contribution of genetic variability in the differential robustness, intensity and response composition, observed between embryo clutches.

Retinoic acid signaling changes due to environmental changes and disease risk

RA levels are tightly regulated throughout life at multiple levels to prevent aberrant signaling and as a consequence, abnormal gene expression as a result of diet and other environmental insults (Blaner, 2019; Blaner et al., 2016; Ghyselinck and Duester, 2019; Kedishvili, 2016; Coberly et al., 1996; Lie et al., 2019; Paganelli et al., 2010; Shabtai et al., 2018). During early embryogenesis, when RA biosynthesis initiates and it is restricted to a limited repertoire of metabolic enzymes, this regulation is particularly important and susceptible to changes.

For several decades, retinoic acid signaling has been the focus of intensive study due to the severe teratogenic effects of abnormal levels and its involvement in the regulation of numerous embryonic processes, oncogenes, and other signaling pathways. While the exposure of embryos or cells to RA induces dramatic developmental changes and malformations, treatment of the same embryos with retinol, the RA precursor, requires much higher concentrations (~100X) to induce similar defects (Durston et al., 1989). Several models could

explain the different teratogenic potential of the precursor (retinol) or its final product (RA). In both instances, members of the CYP26 family of cytochrome P450 enzymes should partially neutralize the RA added or produced (Dobbs-McAuliffe et al., 2004; Duester et al., 2003; Hollemann et al., 1998; Sakai et al., 2001). The main difference then becomes the fact that retinol has to go through RA biosynthesis while RA is already the final active signaling ligand (Duester, 2008; Kedishvili, 2016; Parés et al., 2008). The oxidation of retinol to retinaldehyde is a reversible reaction which can reduce substrate availability for the ALDH enzymes. On the other hand, treatment with RA can only be countered through inactivation by CYP26 enzymes. Therefore, the reduced teratogenic efficacy of the retinol treatment could be the result of reduced conversion to RA as part of the feedback regulation of this network, i.e. robustness, while RA treatment is very restricted in its robustness response.

We obtained evidence of the RA signaling robustness employing several experimental approaches. In all instances, we observed a fast response to the RA manipulation such that at the transcriptome level, the treated samples were not significantly different from controls. All our experiments were performed by either partially inhibiting the endogenous levels of RA, or by slightly increasing (about 10% increase) the physiological content of RA in the embryo. Under these conditions, the RA robustness of the embryo efficiently regulates and normalizes the transcriptome as a whole via feedback. Based on the comparative analysis of the 12 clutches (genetic backgrounds), we can suggest that robustness efficiency will have a threshold beyond which it will become ineffective in restoring normal RA signaling. Our clutch analysis suggests that this threshold might be strongly dependent on genetic polymorphisms affecting enzymatic activity or gene expression parameters. In support, a threshold or toxicological tipping point for RA signaling was recently described in a cell-based model (Saili et al., 2019). The clutch analysis also showed that the network response, i.e. the genes actually up- or down-regulated, is also dependent on genetic variability like promoter polymorphisms. Then, the

developmental malformations arising from environmental insults on RA signaling largely depend on genetic polymorphisms which will determine the efficiency and threshold of the response and the actual network components comprising such a response.

MATERIALS AND METHODS

Embryo culture

Xenopus laevis frogs were purchased from Xenopus I or NASCO (Dexter, MI or Fort Atkinson, WI). Experiments were performed after approval and under the supervision of the Institutional Animal Care and Use Committee (IACUC) of the Hebrew University (Ethics approval no. MD-17-15281-3). Embryos were obtained by *in vitro* fertilization, incubated in 0.1% MBSH and staged according to Nieuwkoop and Faber (Nieuwkoop and Faber, 1967).

Embryo Treatments

all-trans Retinoic acid (RA), Dimethyl sulfoxide (DMSO), and 4-Diethylaminobenzaldehyde (DEAB), were purchased from Sigma-Aldrich (St. Louis, Missouri). Stock solutions of RA, and DEAB, were prepared in DMSO. Two-hour treatments of 10 nM RA, or 50 µM DEAB, were initiated during late blastula (st. 9.5) and terminated at early gastrula (st. 10.25) by three changes of 0.1% MBSH and further incubation in fresh 0.1% MBSH for the desired time.

Total RNA purification from embryos and cDNA preparation

For each sample, 5-10 staged embryos were collected and stored at -80°C. RNA purification was performed using the Bio-Rad Aurum Total RNA Mini Kit (according to the manufacturer's instructions). RNA samples were used for cDNA synthesis using the Bio-Rad iScriptTM Reverse Transcription Supermix for RT-qPCR kit (according to the manufacturer's instructions).

Expression analysis

Quantitative real-time RT-PCR (qPCR) was performed using the Bio-Rad CFX384 thermal cycler and the iTaq Universal SYBR Green Supermix (Bio-Rad). All samples were processed in triplicate and analyzed as described previously(Livak and Schmittgen, 2001). All experiments were repeated with six different embryo batches. qPCR primers used are listed in (Supplemental Table S2).

RNASeq data analysis

Sequencing was performed at the Thomas Jefferson University Genomics Core using Illumina HiSeq 4000. Reads were mapped to the genome using the Xenopus laevis 9.1 genome with STAR alignment and a modified BLAST and FASTQC in the NGS pipeline (STAR average mapped length: 142.34). Annotation of the mapped sequences using *verse* identified 31535 genes. Raw counts were further filtered for non-zero variance across all samples resulting in 31440 scaffold IDs.

High throughput qPCR

cDNA samples were directly processed for reverse transcriptase reaction using SuperScript VILO Master Mix (Thermo Fisher Scientific, Waltham, MA), followed by real-time PCR for targeted amplification and detection using the Evagreen intercalated dye-based approach to detect the PCR-amplified product.

Intron-spanning PCR primers were designed for every assay using Primer3 and BLAST for 24 genes from Retinoic Acid metabolism and target pathway (Supplemental Table S2). The standard BioMark protocol was used to preamplify cDNA samples for 22 cycles using TaqMan PreAmp Master Mix as per the manufacturer's protocol (Applied Biosystems, Foster City, CA, USA). qPCR reactions were performed using 96.96 BioMark Dynamic Arrays (Fluidigm, South San Francisco, CA, USA) enabling quantitative measurement of multiple mRNAs and

samples under identical reaction conditions. Each run consisted of 30 amplification cycles (15 s at 95°C, 5 s at 70°C, 60 s at 60°C). Ct values were calculated by the Real-Time PCR Analysis Software (Fluidigm). Samples were run in triplicate for the 24 genes. The primers in the first pre-amplification group selectively bind for the long isoforms of the genes. In the second pre-amplification group, primers were selected for the short isoforms only. Third pre-amplification group binds to all the 24 genes. In order to remove the technical variability caused due to long and short isoform of the genes, Ct value for each gene in a sample was selected as the median value of the three pre-amplification runs. Relative gene expression was determined by the ΔΔCt method. Gapdh was used as a housekeeping gene for normalization of the data.

Data normalization and annotation

Data analysis on raw genes count was performed using the R statistical analysis tool version 3.6.0 on a 64-bit Windows platform. For the RNA-seq data, the raw genes counts were first converted into log2-transformed values using the "regularized log (rlog)" transformation from the DESeq2 package, which minimizes differences between samples for rows with small counts (Love et al., 2014). The gene expression data was then normalized across samples against the experimental variation and batch effects using COMBAT method in R using a non-parametric adjustment (Johnson et al., 2007). Following batch correction, the gene list was filtered for a minimum expression threshold to remove genes with normalized count less than 5 across all 72 samples. The expression data for the remaining genes was normalized using quantile normalization**.** RNA-Seq transcript/array probes IDs were transformed to Official Gene Symbol using merged list from 3 sources: the Xenopus laevis scaffold-gene mapping, DAVID Bioinformatics Resource 6.8 (Huang et al., 2009) or AnnotationData package "org.Xl.eg.db" maintained by Bioconductor (Carlson, 2017). The original scaffold IDs were retained along with the Official Gene Symbols for cross-reference purposes.

Differential gene expression analysis

The normalized data was analyzed using an Empirical Bayes Statistical (eBayes) model that considered the following two variables and their interactions: (1) Treatment (Control, RA, DEAB) and (2) Time post treatment-washout (t = 0, 1.5, 3, 4.5h). Differentially expressed genes were identified based on statistically significant effects of Time, Treatment or an interaction between these two factors. P-values were adjusted for multiple testing using topTable from *limma* (Ritchie et al., 2015) package in R ($q \leq 0.05$). The significance-filtered differential gene expression data was used in an established Principal Component Analysis (PCA) approach using the *prcomp* function implemented in R. The samples were annotated based on a combination of treatment and time, yielding 12 distinct sample groups. For each of the selected PC, expression of 100 top positively-loaded and 100 top negatively-loaded genes was visualized using a heat map.

Dynamic pattern analysis and COMPACT analysis

First, for each time point for each of the treatment conditions, the gene expression data for all six clutches (A,B,C,D,E,F) was averaged. Within treatment groups RA, DEAB, Control, the gene expression data at time points t=1.5, 3, 4.5h was normalized by subtracting the corresponding 't=0h' group. This average differential gene expression data was then discretized to three levels (+1, 0, −1) based on a fold-change threshold [±2 (up, no or down-regulation)]. Within the three treatment groups, this discretization yielded a dynamic response pattern vector for each gene, encoded by one of 27 (3 levels^3 time-points) possible ordered sets. Counts of genes in each treatment group that follow each of the 27 * 27 (=729) possibilities were compared. Functional enrichment analysis was performed for geneset in various dynamic pattern vectors in the Control conditions, using functions *enrichGO* and *simplify* from the R package "clusterProfiler" (Yu et al., 2012).

COMPACT analysis of RA and DEAB after normalizing to Control

First, for each time point for each of the treatment conditions, the gene expression data for all six clutches (A,B,C,D,E,F) was averaged. Within treatment groups RA and DEAB, the gene expression data were normalized to Control at each time point by subtracting the expression of the Control group at the corresponding time point. This Control-normalized differential gene expression data for both treatment groups was then discretized to three levels (+1, 0, −1) based on a fold-change threshold [±log2(1.3) (up, no or down- regulation)]. This discretization yielded a dynamic response pattern vector for each gene, encoded by one of 81 (3 levels^4 time-points) possible ordered sets. Subsequently, RA and DEAB groups were compared to count the number of genes corresponding to each of the 81 * 81 (=6561) possibilities; to create a 81 × 81 matrix representing the comparative dynamic response pattern counts (COMPACT) (Kuttippurathu et al., 2016). For a given COMPACT matrix of comparative conditions RA(vs. Control) and DEAB (vs. Control), the element at the ith row and jth column of the matrix contains the number of genes that show an 'i'th pattern in DEAB and 'j'th pattern in RA. For a coarse-grained version of the detailed 81x81 COMPACT, pattern-vector counts for each treatment group were further aggregated based on the first time-point, yielding 9 groups of pattern vectors per treatment group. The pair of treatment group (RA and DEAB) was then compared to count the number of genes corresponding to each of the 9 * 9 (=81) possibilities.

RA network map and visualization

A schematic representation for the position and functioning of the genes involved in the RA biosynthesis, metabolism, translocation and transcription was formulated from the literature. For each time point for each treatment, expression value for each gene was mapped to the corresponding label in the schematics using a color scale.

Gene correlation and clustering analysis - Gene expression data was analysed for both with and without Control-normalization using Weighted Gene Coexpression Network Analysis (WGCNA) (Langfelder and Horvath, 2008) to identify modules of genes with highly correlated

differential expression. We used a soft threshold value of 9 (8 for Control normalized data) to identify the initial gene coexpression modules, followed by a dissimilarity threshold of 0.25 to merge the initial modules into the final set of gene coexpression modules. Identified modules were further correlated with the traits (batch, time, treatment).

Robustness score calculation and principal curve-based trajectory analysis

RNA-seq expression data of (clutches: A,B,C,D,E,F) and additional normalized qPCR expression data (clutches: G,H,I,J,K,L) were independently genewise Z-score transformed. Transformed data was then combined to result into 144 samples (12 clutches * 3 treatments * 4 timepoints). We further selected two subsets of genes: 1) "RA metabolism genes" [aldh1a2.L, aldh1a3.L, crabp2.L, crabp2.S, cyp26a1.L, cyp26a1.S, cyp26c1.L, cyp26c1.S, dhrs3.L, rbp1.L, rdh10.L, rdh10.S, rdh13.L, rdh14.L, sdr16c5.L, stra6.L]. This set represents the feedback regulatory mechanism utilised in response to the RA levels perturbations. 2) "HOX genes" [hoxa1.L, hoxa1.S, hoxa3.S, hoxb1.S, hoxb4.S, hoxd4.L] representing the phenotypic outcome from the treatment. For each gene set, the PCA scores for the combined data was first calculated using R function *prcomp* and then the scores from the first three principal components (PC1, PC2 and PC3) are used to learn a 3-dimensional principal curve using the function *principal_curve* from R package princurve. Two sets of points are specified for the 'start' parameter for this function, which determines the origin and direction of the curve: (1) The centroid of the 0h-Control samples from all twelve clutches, and (2) centroid of all the remaining 132 samples. For each geneset (RA metabolism genes and HOX genes), for each clutch (A-L), for each treatment (RA or DEAB), a "net absolute expression shift" can be calculated as the sum of distances along the principal curve, of the treatment samples from the corresponding control samples:

$$s.hox_{cl}^{RA} = \sum_{t} \quad abs\left(\frac{\lambda.hox_{cl}^{RA(t)} - \lambda.hox_{cl}^{Control(t)}}{max(\lambda.hox)}\right)$$

where, $\lambda.hox_{cl}^{RA(t)}$ is the arc-distance from the beginning of the curve, for the "*RA treatment samples*" at time point "*t*", for clutch "*cl*" for the principal curve learned for the geneset "*Hox genes*" (Returned as the parameter "*lambda*" from the principal curve function). The expression shift calculation allows ranking and sorting clutches along measures 'HOX shift' ($s.hox_{cl}^{treatment}$) and 'RA Network shift' ($s.metabolism_{cl}^{treatment}$). A higher HOX shift for a clutch for a treatment indicates that the clutch is more robust to that particular treatment/perturbation. Furthermore, clutches were mapped onto the conceptual map across the spectrum of "HOX shift" and "RA Network shift" divided into hypothetical quadrants of Effective or Ineffective regulation, or Efficient or Inefficient regulation.

Availability of supporting data/additional files

The raw and normalized datasets for the RNAseq and HT-qPCR data are available online as Gene Expression Omnibus datasets via SuperSeries GSE154408 containing RNAseq data: GSE154399 and HT-qPCR data: GSE154407.

FUNDING

RV acknowledges financial support for the project from the National Institute of Biomedical Imaging and Bioengineering grant U01 EB023224 and from the Department of Pathology, Anatomy, and Cell Biology, Thomas Jefferson University. AF acknowledges financial support from the Israel Science Foundation (grant 668/17) and the Wolfson Family Chair in Genetics. RV and AF acknowledge the Pilot Funding grant from Thomas Jefferson University and The Hebrew University of Jerusalem collaborative research program.

ABBREVIATIONS USED

COMPACT: Comparative Matrix of Pattern Counts

DEAB: 4-diethylaminobenzaldehyde

PCA: Principal Component Analysis

PCR: Polymerase Chain Reaction

RA: retinoic acid

WGCNA: Weighted Gene Coexpression Network Analysis

AUTHOR CONTRIBUTIONS

R.V. and A.F. conceived and supervised the study and designed the experiments and analysis methodology. L.B-K., M.G., K.K., and A.F. performed embryo experiments and real-time PCR assessment and developed the figures. A.B. performed the initial analysis of the RNAseq data. S.A. conducted the high-throughput PCR validation of RNAseq results. M.P. conducted the analysis of transcriptomics and HT-qPCR data and performed the network and trajectory analyses and developed the figures. M.P., R.V., and A.F. interpreted the results and drafted the manuscript.

ETHICS DECLARATIONS

The authors declare no competing interests.

BIBLIOGRAPHY

Adams, M.K., Belyaeva, O.V., Wu, L., Kedishvili, N.Y., 2014. The retinaldehyde reductase activity of DHRS3 is reciprocally activated by retinol dehydrogenase 10 to control retinoid homeostasis. J. Biol. Chem. 289, 14868–14880. doi:10.1074/jbc.M114.552257

Begemann, G., Schilling, T.F., Rauch, G.J., Geisler, R., Ingham, P.W., 2001. The zebrafish neckless mutation reveals a requirement for raldh2 in mesodermal signals that pattern the hindbrain. Development 128, 3081–3094.

Belyaeva, O.V., Adams, M.K., Wu, L., Kedishvili, N.Y., 2017. The antagonistically bifunctional retinoid oxidoreductase complex is required for maintenance of all-trans-retinoic acid homeostasis. J. Biol. Chem. 292, 5884–5897. doi:10.1074/jbc.M117.776914

Belyaeva, O.V., Korkina, O.V., Stetsenko, A.V., Kedishvili, N.Y., 2008. Human retinol dehydrogenase 13 (RDH13) is a mitochondrial short-chain dehydrogenase/reductase with a retinaldehyde reductase activity. FEBS J. 275, 138–147. doi:10.1111/j.1742-4658.2007.06184.x

Billings, S.E., Pierzchalski, K., Butler Tjaden, N.E., Pang, X.-Y., Trainor, P.A., Kane, M.A., Moise, A.R., 2013. The retinaldehyde reductase DHRS3 is essential for preventing the formation of excess retinoic acid during embryonic development. FASEB J. 27, 4877–4889. doi:10.1096/fj.13-227967

Blaner, W.S., 2019. Vitamin A signaling and homeostasis in obesity, diabetes, and metabolic disorders. Pharmacol. Ther. 197, 153–178. doi:10.1016/j.pharmthera.2019.01.006

Blaner, W.S., Li, Y., Brun, P.-J., Yuen, J.J., Lee, S.-A., Clugston, R.D., 2016. Vitamin A absorption, storage and mobilization. Subcell Biochem 81, 95–125. doi:10.1007/978-94-024-0945-1_4

Blentic, A., Gale, E., Maden, M., 2003. Retinoic acid signalling centres in the avian embryo identified by sites of expression of synthesising and catabolising enzymes. Dev. Dyn. 227, 114–127. doi:10.1002/dvdy.10292

Blumberg, B., Bolado, J., Moreno, T.A., Kintner, C., Evans, R.M., Papalopulu, N., 1997. An essential role for retinoid signaling in anteroposterior neural patterning. Development 124, 373–379.

Boehm, S.L., Lundahl, K.R., Caldwell, J., Gilliam, D.M., 1997. Ethanol teratogenesis in the C57BL/6J, DBA/2J and A/J inbred mouse strains. Alcohol 14, 389–395.

Borel, P., Desmarchelier, C., 2017. Genetic Variations Associated with Vitamin A Status and Vitamin A Bioavailability. Nutrients 9. doi:10.3390/nu9030246

Campo-Paysaa, F., Marlétaz, F., Laudet, V., Schubert, M., 2008. Retinoic acid signaling in development: tissue-specific functions and evolutionary origins. Genesis 46, 640–656. doi:10.1002/dvg.20444

Carlson, M., 2017. org.Xl.eg.db. Bioconductor. doi:10.18129/b9.bioc.org.xl.eg.db

Chen, Y., Pollet, N., Niehrs, C., Pieler, T., 2001. Increased XRALDH2 activity has a posteriorizing effect on the central nervous system of Xenopus embryos. Mech. Dev. 101, 91–103. doi:10.1016/S0925-4773(00)00558-X

Clagett-Dame, M., DeLuca, H.F., 2002. The role of vitamin A in mammalian reproduction and embryonic development. Annu. Rev. Nutr. 22, 347–381.

doi:10.1146/annurev.nutr.22.010402.102745E
Clagett-Dame, M., Knutson, D., 2011. Vitamin A in reproduction and development. Nutrients 3, 385–428. doi:10.3390/nu3040385
Coberly, S., Lammer, E., Alashari, M., 1996. Retinoic acid embryopathy: case report and review of literature. Pediatric Pathology & Laboratory Medicine 16, 823–836. doi:10.1080/15513819609169308
Collins, M.D., Mao, G.E., 1999. Teratology of retinoids. Annu. Rev. Pharmacol. Toxicol. 39, 399–430. doi:10.1146/annurev.pharmtox.39.1.399
Cui, J., Michaille, J.-J., Jiang, W., Zile, M.H., 2003. Retinoid receptors and vitamin A deficiency: differential patterns of transcription during early avian development and the rapid induction of RARs by retinoic acid. Dev. Biol. 260, 496–511.
Cunningham, T.J., Duester, G., 2015. Mechanisms of retinoic acid signalling and its roles in organ and limb development. Nat. Rev. Mol. Cell Biol. 16, 110–123. doi:10.1038/nrm3932
D'Aniello, E., Rydeen, A.B., Anderson, J.L., Mandal, A., Waxman, J.S., 2013. Depletion of retinoic acid receptors initiates a novel positive feedback mechanism that promotes teratogenic increases in retinoic acid. PLoS Genet. 9, e1003689. doi:10.1371/journal.pgen.1003689
D'Aniello, E., Waxman, J.S., 2015. Input overload: Contributions of retinoic acid signaling feedback mechanisms to heart development and teratogenesis. Dev. Dyn. 244, 513–523. doi:10.1002/dvdy.24232
Dobbs-McAuliffe, B., Zhao, Q., Linney, E., 2004. Feedback mechanisms regulate retinoic acid production and degradation in the zebrafish embryo. Mech. Dev. 121, 339–350. doi:10.1016/j.mod.2004.02.008
Dubey, A., Rose, R.E., Jones, D.R., Saint-Jeannet, J.-P., 2018. Generating retinoic acid gradients by local degradation during craniofacial development: One cell's cue is another cell's poison. Genesis 56. doi:10.1002/dvg.23091
Duester, G., 1991. A hypothetical mechanism for fetal alcohol syndrome involving ethanol inhibition of retinoic acid synthesis at the alcohol dehydrogenase step. Alcohol. Clin. Exp. Res. 15, 568–572. doi:10.1111/j.1530-0277.1991.tb00562.x
Duester, G., 2008. Retinoic acid synthesis and signaling during early organogenesis. Cell 134, 921–931. doi:10.1016/j.cell.2008.09.002
Duester, G., Mic, F.A., Molotkov, A., 2003. Cytosolic retinoid dehydrogenases govern ubiquitous metabolism of retinol to retinaldehyde followed by tissue-specific metabolism to retinoic acid. Chem Biol Interact 143–144, 201–210.
Durston, A.J., Timmermans, J.P., Hage, W.J., Hendriks, H.F., de Vries, N.J., Heideveld, M., Nieuwkoop, P.D., 1989. Retinoic acid causes an anteroposterior transformation in the developing central nervous system. Nature 340, 140–144. doi:10.1038/340140a0
Eberhart, J.K., Parnell, S.E., 2016. The genetics of fetal alcohol spectrum disorders. Alcohol. Clin. Exp. Res. 40, 1154–1165. doi:10.1111/acer.13066
Eldar, A., Shilo, B.-Z., Barkai, N., 2004. Elucidating mechanisms underlying robustness of morphogen gradients. Curr. Opin. Genet. Dev. 14, 435–439. doi:10.1016/j.gde.2004.06.009
El Kares, R., Manolescu, D.C., Lakhal-Chaieb, L., Montpetit, A., Zhang, Z., Bhat, P.V.,

Goodyer, P., 2010. A human ALDH1A2 gene variant is associated with increased newborn kidney size and serum retinoic acid. Kidney Int. 78, 96–102. doi:10.1038/ki.2010.101

Evans, B.J., Kwon, T., 2015. Molecular polymorphism and divergence of duplicated genes in tetraploid african clawed frogs (xenopus). Cytogenet. Genome Res. 145, 243–252. doi:10.1159/000431108

Feng, L., Hernandez, R.E., Waxman, J.S., Yelon, D., Moens, C.B., 2010. Dhrs3a regulates retinoic acid biosynthesis through a feedback inhibition mechanism. Dev. Biol. 338, 1–14. doi:10.1016/j.ydbio.2009.10.029

Fujii, H., Sato, T., Kaneko, S., Gotoh, O., Fujii-Kuriyama, Y., Osawa, K., Kato, S., Hamada, H., 1997. Metabolic inactivation of retinoic acid by a novel P450 differentially expressed in developing mouse embryos. EMBO J. 16, 4163–4173. doi:10.1093/emboj/16.14.4163

Ghyselinck, N.B., Duester, G., 2019. Retinoic acid signaling pathways. Development 146. doi:10.1242/dev.167502

Grandel, H., Lun, K., Rauch, G.-J., Rhinn, M., Piotrowski, T., Houart, C., Sordino, P., Küchler, A.M., Schulte-Merker, S., Geisler, R., Holder, N., Wilson, S.W., Brand, M., 2002. Retinoic acid signalling in the zebrafish embryo is necessary during pre-segmentation stages to pattern the anterior-posterior axis of the CNS and to induce a pectoral fin bud. Development 129, 2851–2865.

Green, R.F., Stoler, J.M., 2007. Alcohol dehydrogenase 1B genotype and fetal alcohol syndrome: a HuGE minireview. Am. J. Obstet. Gynecol. 197, 12–25. doi:10.1016/j.ajog.2007.02.028

Hartomo, T.B., Van Huyen Pham, T., Yamamoto, N., Hirase, S., Hasegawa, D., Kosaka, Y., Matsuo, M., Hayakawa, A., Takeshima, Y., Iijima, K., Nishio, H., Nishimura, N., 2015. Involvement of aldehyde dehydrogenase 1A2 in the regulation of cancer stem cell properties in neuroblastoma. Int. J. Oncol. 46, 1089–1098. doi:10.3892/ijo.2014.2801

Hollemann, T., Chen, Y., Grunz, H., Pieler, T., 1998. Regionalized metabolic activity establishes boundaries of retinoic acid signalling. EMBO J. 17, 7361–7372. doi:10.1093/emboj/17.24.7361

Huang, D.W., Sherman, B.T., Lempicki, R.A., 2009. Systematic and integrative analysis of large gene lists using DAVID bioinformatics resources. Nat. Protoc. 4, 44–57. doi:10.1038/nprot.2008.211

Janesick, A., Abbey, R., Chung, C., Liu, S., Taketani, M., Blumberg, B., 2013. ERF and ETV3L are retinoic acid-inducible repressors required for primary neurogenesis. Development 140, 3095–3106. doi:10.1242/dev.093716

Janesick, A., Nguyen, T.T.L., Aisaki, K., Igarashi, K., Kitajima, S., Chandraratna, R.A.S., Kanno, J., Blumberg, B., 2014. Active repression by RARγ signaling is required for vertebrate axial elongation. Development 141, 2260–2270. doi:10.1242/dev.103705

Janesick, A., Wu, S.C., Blumberg, B., 2015. Retinoic acid signaling and neuronal differentiation. Cell. Mol. Life Sci. 72, 1559–1576. doi:10.1007/s00018-014-1815-9

Johnson, W.E., Li, C., Rabinovic, A., 2007. Adjusting batch effects in microarray expression data using empirical Bayes methods. Biostatistics 8, 118–127. doi:10.1093/biostatistics/kxj037

Jones, K.L., Smith, D.W., Ulleland, C.N., Streissguth, P., 1973. Pattern of malformation in offspring of chronic alcoholic mothers. Lancet 1, 1267–1271. doi:10.1016/s0140-6736(73)91291-9

Kam, R.K.T., Shi, W., Chan, S.O., Chen, Y., Xu, G., Lau, C.B.-S., Fung, K.P., Chan, W.Y., Zhao, H., 2013. Dhrs3 protein attenuates retinoic acid signaling and is required for early embryonic patterning. J. Biol. Chem. 288, 31477–31487. doi:10.1074/jbc.M113.514984

Kedishvili, N.Y., 2013. Enzymology of retinoic acid biosynthesis and degradation. J. Lipid Res. 54, 1744–1760. doi:10.1194/jlr.R037028

Kedishvili, N.Y., 2016. Retinoic acid synthesis and degradation. Subcell Biochem 81, 127–161. doi:10.1007/978-94-024-0945-1_5

Kessel, M., 1992. Respecification of vertebral identities by retinoic acid. Development 115, 487–501.

Kim, H., Lapointe, J., Kaygusuz, G., Ong, D.E., Li, C., van de Rijn, M., Brooks, J.D., Pollack, J.R., 2005. The retinoic acid synthesis gene ALDH1a2 is a candidate tumor suppressor in prostate cancer. Cancer Res. 65, 8118–8124. doi:10.1158/0008-5472.CAN-04-4562

Koide, T., Downes, M., Chandraratna, R.A., Blumberg, B., Umesono, K., 2001. Active repression of RAR signaling is required for head formation. Genes Dev. 15, 2111–2121. doi:10.1101/gad.908801

Kono, N., Arai, H., 2015. Intracellular transport of fat-soluble vitamins A and E. Traffic 16, 19–34. doi:10.1111/tra.12231

Koren, G., 2012. The first description of fetal alcohol syndrome by French pediatrician Paul Lemoine. J. Popul. Ther. Clin. Pharmacol. 19, e223.

Kot-Leibovich, H., Fainsod, A., 2009. Ethanol induces embryonic malformations by competing for retinaldehyde dehydrogenase activity during vertebrate gastrulation. Dis. Model. Mech. 2, 295–305. doi:10.1242/dmm.001420

Kraft, J.C., Juchau, M.R., 1992. Correlations between conceptal concentrations of all-trans-retinoic acid and dysmorphogenesis after microinjections of all-trans-retinoic acid, 13-cis-retinoic acid, all-trans-retinoyl-beta-glucuronide, or retinol in cultured whole rat embryos. Drug Metab. Dispos. 20, 218–225.

Kraft, J.C., Kimelman, D., Juchau, M.R., 1995. Xenopus laevis: a model system for the study of embryonic retinoid metabolism. I. Embryonic metabolism of 9-cis- and all-trans-retinals and retinols to their corresponding acid forms. Drug Metab. Dispos. 23, 72–82.

Kuttippurathu, L., Juskeviciute, E., Dippold, R.P., Hoek, J.B., Vadigepalli, R., 2016. A novel comparative pattern analysis approach identifies chronic alcohol mediated dysregulation of transcriptomic dynamics during liver regeneration. BMC Genomics 17, 260. doi:10.1186/s12864-016-2492-x

Langfelder, P., Horvath, S., 2008. WGCNA: an R package for weighted correlation network analysis. BMC Bioinformatics 9, 559. doi:10.1186/1471-2105-9-559

Lee, L.M.Y., Leung, C.-Y., Tang, W.W.C., Choi, H.-L., Leung, Y.-C., McCaffery, P.J., Wang, C.-C., Woolf, A.S., Shum, A.S.W., 2012. A paradoxical teratogenic mechanism for retinoic acid. Proc Natl Acad Sci USA 109, 13668–13673. doi:10.1073/pnas.1200872109

Leibovich, A., Edri, T., Klein, S.L., Moody, S.A., Fainsod, A., 2020. Natural size variation

among embryos leads to the corresponding scaling in gene expression. Dev. Biol. 462, 165–179. doi:10.1016/j.ydbio.2020.03.014

Lemoine, P., Harousseau, H., Borteyru, J.P., Menuet, J.C., 1968. Les enfants de parents alcooliques: Anomalies observees a propos de 127 cas. Ouest méd 8, 476–482.

le Maire, A., Bourguet, W., 2014. Retinoic acid receptors: structural basis for coregulator interaction and exchange. Subcell Biochem 70, 37–54. doi:10.1007/978-94-017-9050-5_3

Lie, K.K., Meier, S., Sørhus, E., Edvardsen, R.B., Karlsen, Ø., Olsvik, P.A., 2019. Offshore crude oil disrupts retinoid signaling and eye development in larval atlantic haddock. Front. Mar. Sci. 6. doi:10.3389/fmars.2019.00368

Livak, K.J., Schmittgen, T.D., 2001. Analysis of relative gene expression data using real-time quantitative PCR and the 2(-Delta Delta C(T)) Method. Methods 25, 402–408. doi:10.1006/meth.2001.1262

Lohnes, D., Mark, M., Mendelsohn, C., Dollé, P., Decimo, D., LeMeur, M., Dierich, A., Gorry, P., Chambon, P., 1995. Developmental roles of the retinoic acid receptors. J. Steroid Biochem. Mol. Biol. 53, 475–486.

Loucks, E., Carvan, M.J., 2004. Strain-dependent effects of developmental ethanol exposure in zebrafish. Neurotoxicol. Teratol. 26, 745–755. doi:10.1016/j.ntt.2004.06.017

Love, M.I., Huber, W., Anders, S., 2014. Moderated estimation of fold change and dispersion for RNA-seq data with DESeq2. Genome Biol. 15, 550. doi:10.1186/s13059-014-0550-8

Lupo, G., Liu, Y., Qiu, R., Chandraratna, R.A.S., Barsacchi, G., He, R.-Q., Harris, W.A., 2005. Dorsoventral patterning of the Xenopus eye: a collaboration of Retinoid, Hedgehog and FGF receptor signaling. Development 132, 1737–1748. doi:10.1242/dev.01726

Marill, J., Idres, N., Capron, C.C., Nguyen, E., Chabot, G.G., 2003. Retinoic acid metabolism and mechanism of action: a review. Curr Drug Metab 4, 1–10.

Mark, M., Ghyselinck, N.B., Chambon, P., 2009. Function of retinoic acid receptors during embryonic development. Nucl. Recept. Signal. 7, e002. doi:10.1621/nrs.07002

Mendelsohn, C., Lohnes, D., Décimo, D., Lufkin, T., LeMeur, M., Chambon, P., Mark, M., 1994. Function of the retinoic acid receptors (RARs) during development (II). Multiple abnormalities at various stages of organogenesis in RAR double mutants. Development 120, 2749–2771.

Metzler, M.A., Sandell, L.L., 2016. Enzymatic metabolism of vitamin A in developing vertebrate embryos. Nutrients 8, pii: E812. doi:10.3390/nu8120812

Michiue, T., Yamamoto, T., Yasuoka, Y., Goto, T., Ikeda, T., Nagura, K., Nakayama, T., Taira, M., Kinoshita, T., 2017. High variability of expression profiles of homeologous genes for Wnt, Hh, Notch, and Hippo signaling pathways in Xenopus laevis. Dev. Biol. 426, 270–290. doi:10.1016/j.ydbio.2016.12.006

Napoli, J.L., 2016. Functions of Intracellular Retinoid Binding-Proteins. Subcell Biochem 81, 21–76. doi:10.1007/978-94-024-0945-1_2

Napoli, J.L., 2017. Cellular retinoid binding-proteins, CRBP, CRABP, FABP5: Effects on retinoid metabolism, function and related diseases. Pharmacol. Ther. 173, 19–33. doi:10.1016/j.pharmthera.2017.01.004

Niederreither, K., Abu-Abed, S., Schuhbaur, B., Petkovich, M., Chambon, P., Dollé, P., 2002. Genetic evidence that oxidative derivatives of retinoic acid are not involved in retinoid signaling during mouse development. Nat. Genet. 31, 84–88. doi:10.1038/ng876

Niederreither, K., McCaffery, P., Dräger, U.C., Chambon, P., Dollé, P., 1997. Restricted expression and retinoic acid-induced downregulation of the retinaldehyde dehydrogenase type 2 (RALDH-2) gene during mouse development. Mech. Dev. 62, 67–78. doi:10.1016/S0925-4773(96)00653-3

Niederreither, K., Subbarayan, V., Dollé, P., Chambon, P., 1999. Embryonic retinoic acid synthesis is essential for early mouse post-implantation development. Nat. Genet. 21, 444–448. doi:10.1038/7788

Nieuwkoop, P.D., Faber, J., 1967. Normal table of Xenopus laevis (Daudin): A systematical and chronological survey of the development from the fertilized egg till the end of metamorphosis. North-Holland Publishing Company, Amsterdam.

Nijhout, H.F., Best, J.A., Reed, M.C., 2019. Systems biology of robustness and homeostatic mechanisms. Wiley Interdiscip. Rev. Syst. Biol. Med. 11, e1440. doi:10.1002/wsbm.1440

O'Byrne, S.M., Blaner, W.S., 2013. Retinol and retinyl esters: biochemistry and physiology. J. Lipid Res. 54, 1731–1743. doi:10.1194/jlr.R037648

Paganelli, A., Gnazzo, V., Acosta, H., López, S.L., Carrasco, A.E., 2010. Glyphosate-based herbicides produce teratogenic effects on vertebrates by impairing retinoic acid signaling. Chem. Res. Toxicol. 23, 1586–1595. doi:10.1021/tx1001749

Pangilinan, F., Molloy, A.M., Mills, J.L., Troendle, J.F., Parle-McDermott, A., Kay, D.M., Browne, M.L., McGrath, E.C., Abaan, H.O., Sutton, M., Kirke, P.N., Caggana, M., Shane, B., Scott, J.M., Brody, L.C., 2014. Replication and exploratory analysis of 24 candidate risk polymorphisms for neural tube defects. BMC Med. Genet. 15, 102. doi:10.1186/s12881-014-0102-9

Parés, X., Farrés, J., Kedishvili, N., Duester, G., 2008. Medium- and short-chain dehydrogenase/reductase gene and protein families : Medium-chain and short-chain dehydrogenases/reductases in retinoid metabolism. Cell. Mol. Life Sci. 65, 3936–3949. doi:10.1007/s00018-008-8591-3

Porté, S., Xavier Ruiz, F., Giménez, J., Molist, I., Alvarez, S., Domínguez, M., Alvarez, R., de Lera, A.R., Parés, X., Farrés, J., 2013. Aldo-keto reductases in retinoid metabolism: search for substrate specificity and inhibitor selectivity. Chem. Biol. Interact. 202, 186–194. doi:10.1016/j.cbi.2012.11.014

Pullarkat, R.K., 1991. Hypothesis: prenatal ethanol-induced birth defects and retinoic acid. Alcohol. Clin. Exp. Res. 15, 565–567. doi:10.1111/j.1530-0277.1991.tb00561.x

Reijntjes, S., Blentic, A., Gale, E., Maden, M., 2005. The control of morphogen signalling: regulation of the synthesis and catabolism of retinoic acid in the developing embryo. Dev. Biol. 285, 224–237. doi:10.1016/j.ydbio.2005.06.019

Ritchie, M.E., Phipson, B., Wu, D., Hu, Y., Law, C.W., Shi, W., Smyth, G.K., 2015. limma powers differential expression analyses for RNA-sequencing and microarray studies. Nucleic Acids Res. 43, e47. doi:10.1093/nar/gkv007

Romand, R., Niederreither, K., Abu-Abed, S., Petkovich, M., Fraulob, V., Hashino, E., Dollé, P., 2004. Complementary expression patterns of retinoid acid-synthesizing and -

metabolizing enzymes in pre-natal mouse inner ear structures. Gene Expr. Patterns 4, 123–133. doi:10.1016/j.modgep.2003.09.006

Rydeen, A., Voisin, N., D'Aniello, E., Ravisankar, P., Devignes, C.-S., Waxman, J.S., 2015. Excessive feedback of Cyp26a1 promotes cell non-autonomous loss of retinoic acid signaling. Dev. Biol. 405, 47–55. doi:10.1016/j.ydbio.2015.06.008

Saili, K.S., Antonijevic, T., Zurlinden, T.J., Shah, I., Deisenroth, C., Knudsen, T.B., 2019. Molecular characterization of a toxicological tipping point during human stem cell differentiation. Reprod. Toxicol. 91, 1–13. doi:10.1016/j.reprotox.2019.10.001

Sakai, Y., Meno, C., Fujii, H., Nishino, J., Shiratori, H., Saijoh, Y., Rossant, J., Hamada, H., 2001. The retinoic acid-inactivating enzyme CYP26 is essential for establishing an uneven distribution of retinoic acid along the anterio-posterior axis within the mouse embryo. Genes Dev. 15, 213–225. doi:10.1101/gad.851501

Sandell, L.L., Lynn, M.L., Inman, K.E., McDowell, W., Trainor, P.A., 2012. RDH10 oxidation of Vitamin A is a critical control step in synthesis of retinoic acid during mouse embryogenesis. PLoS ONE 7, e30698. doi:10.1371/journal.pone.0030698

Savova, V., Pearl, E.J., Boke, E., Nag, A., Adzhubei, I., Horb, M.E., Peshkin, L., 2017. Transcriptomic insights into genetic diversity of protein-coding genes in X. laevis. Dev. Biol. 424, 181–188. doi:10.1016/j.ydbio.2017.02.019

Schilling, T.F., Sosnik, J., Nie, Q., 2016. Visualizing retinoic acid morphogen gradients. Methods Cell Biol. 133, 139–163. doi:10.1016/bs.mcb.2016.03.003

Schroeder, F., Petrescu, A.D., Huang, H., Atshaves, B.P., McIntosh, A.L., Martin, G.G., Hostetler, H.A., Vespa, A., Landrock, D., Landrock, K.K., Payne, H.R., Kier, A.B., 2008. Role of fatty acid binding proteins and long chain fatty acids in modulating nuclear receptors and gene transcription. Lipids 43, 1–17. doi:10.1007/s11745-007-3111-z

See, A.W.-M., Kaiser, M.E., White, J.C., Clagett-Dame, M., 2008. A nutritional model of late embryonic vitamin A deficiency produces defects in organogenesis at a high penetrance and reveals new roles for the vitamin in skeletal development. Dev. Biol. 316, 171–190. doi:10.1016/j.ydbio.2007.10.018

Shabtai, Y., Bendelac, L., Jubran, H., Hirschberg, J., Fainsod, A., 2018. Acetaldehyde inhibits retinoic acid biosynthesis to mediate alcohol teratogenicity. Sci. Rep. 8, 347. doi:10.1038/s41598-017-18719-7

Shabtai, Y., Fainsod, A., 2018. Competition between ethanol clearance and retinoic acid biosynthesis in the induction of fetal alcohol syndrome. Biochem. Cell Biol. 96, 148–160. doi:10.1139/bcb-2017-0132

Shabtai, Y., Jubran, H., Nassar, T., Hirschberg, J., Fainsod, A., 2016. Kinetic characterization and regulation of the human retinaldehyde dehydrogenase 2 enzyme during production of retinoic acid. Biochem. J. 473, 1423–1431. doi:10.1042/BCJ20160101

Shabtai, Y., Shukrun, N., Fainsod, A., 2017. ADHFe1: a novel enzyme involved in retinoic acid-dependent Hox activation. Int. J. Dev. Biol. 61, 303–310. doi:10.1387/ijdb.160252af

Sharpe, C.R., Goldstone, K., 1997. Retinoid receptors promote primary neurogenesis in Xenopus. Development 124, 515–523.

Shenefelt, R.E., 1972. Gross congenital malformations. Animal model: treatment of various

species with a large dose of vitamin A at known stages in pregnancy. Am. J. Pathol. 66, 589–592.

Shukrun, N., Shabtai, Y., Pillemer, G., Fainsod, A., 2019. Retinoic acid signaling reduction recapitulates the effects of alcohol on embryo size. Genesis 57, e23284. doi:10.1002/dvg.23284

Sive, H.L., Draper, B.W., Harland, R.M., Weintraub, H., 1990. Identification of a retinoic acid-sensitive period during primary axis formation in Xenopus laevis. Genes Dev. 4, 932–942. doi:10.1101/gad.4.6.932

Sonneveld, E., van den Brink, C.E., van der Leede, B.M., Schulkes, R.K., Petkovich, M., van der Burg, B., van der Saag, P.T., 1998. Human retinoic acid (RA) 4-hydroxylase (CYP26) is highly specific for all-trans-RA and can be induced through RA receptors in human breast and colon carcinoma cells. Cell Growth Differ. 9, 629–637.

Strate, I., Min, T.H., Iliev, D., Pera, E.M., 2009. Retinol dehydrogenase 10 is a feedback regulator of retinoic acid signalling during axis formation and patterning of the central nervous system. Development 136, 461–472. doi:10.1242/dev.024901

Suzuki, A., Yoshida, H., van Heeringen, S.J., Takebayashi-Suzuki, K., Veenstra, G.J.C., Taira, M., 2017. Genomic organization and modulation of gene expression of the TGF-β and FGF pathways in the allotetraploid frog Xenopus laevis. Dev. Biol. 426, 336–359. doi:10.1016/j.ydbio.2016.09.016

Taira, M., Otani, H., Jamrich, M., Dawid, I.B., 1994. Expression of the LIM class homeobox gene Xlim-1 in pronephros and CNS cell lineages of Xenopus embryos is affected by retinoic acid and exogastrulation. Development 120, 1525–1536.

Timoneda, J., Rodríguez-Fernández, L., Zaragozá, R., Marín, M.P., Cabezuelo, M.T., Torres, L., Viña, J.R., Barber, T., 2018. Vitamin A deficiency and the lung. Nutrients 10. doi:10.3390/nu10091132

Urbizu, A., Toma, C., Poca, M.A., Sahuquillo, J., Cuenca-León, E., Cormand, B., Macaya, A., 2013. Chiari malformation type I: a case-control association study of 58 developmental genes. PLoS ONE 8, e57241. doi:10.1371/journal.pone.0057241

Xavier-Neto, J., Sousa Costa, Â.M., Figueira, A.C.M., Caiaffa, C.D., Amaral, F.N. do, Peres, L.M.C., da Silva, B.S.P., Santos, L.N., Moise, A.R., Castillo, H.A., 2015. Signaling through retinoic acid receptors in cardiac development: Doing the right things at the right times. Biochim. Biophys. Acta 1849, 94–111. doi:10.1016/j.bbagrm.2014.08.003

Yelin, R., Schyr, R.B.-H., Kot, H., Zins, S., Frumkin, A., Pillemer, G., Fainsod, A., 2005. Ethanol exposure affects gene expression in the embryonic organizer and reduces retinoic acid levels. Dev. Biol. 279, 193–204. doi:10.1016/j.ydbio.2004.12.014

Yu, G., Wang, L.-G., Han, Y., He, Q.-Y., 2012. clusterProfiler: an R package for comparing biological themes among gene clusters. OMICS 16, 284–287. doi:10.1089/omi.2011.0118

Zhong, G., Ortiz, D., Zelter, A., Nath, A., Isoherranen, N., 2018. CYP26C1 Is a Hydroxylase of Multiple Active Retinoids and Interacts with Cellular Retinoic Acid Binding Proteins. Mol. Pharmacol. 93, 489–503. doi:10.1124/mol.117.111039

FIGURE LEGENDS:

Figure 1. Phenotypic robustness of the retinoic acid metabolic pathway. Retinoic acid levels were manipulated in *Xenopus laevis* embryos. Inhibition of RALDH activity with DEAB or CYP26A1 overexpression to render retinoic acid inactive were utilized to reduce levels of this signal. **(A)** Schematic diagram of the retinoic acid metabolic pathway and the steps affected. **(B)** Control embryo at st. 27. **(C)** Embryo injected with capped RNA (0.8 ng) encoding the CYP26A1 enzyme. A lineage tracer (ß-galactosidase RNA) was included to ensure a dorsal injection. **(D)** Embryo treated with DEAB (50 µM) from the midblastula transition until st. 27. **(E)** Embryo treated with DEAB and injected with *cyp26a1* mRNA.

Figure 2. Retinoic acid manipulation in the physiological range. Embryos were treated with increasing concentrations of all-*trans* RA from 1 nM to 1 µM. Treatments were initiated at the midblastula transition (st. 8.5) and RNA samples were collected at early (st. 10.25) and late (st. 12) gastrula. The response of the RA metabolic and target genes was studied by qPCR. **(A)** *hoxb1* **(B)** *cyp26a1* **(C)** *dhrs3* **(D)** *raldh2* (*aldh1a2*) **(E)** *raldh3* (*aldh1a3*) **(F)** *rdh10*. Statistical significance (Student's t-test) was calculated compared to the expression level in the control group. *, $p<0.05$; **, $p<0.01$; ***, $p<0.001$; ns, not significant.

Figure 3. Kinetics of the recovery from RA manipulation. Embryos were transiently treated with either 10 nM RA (A,B), or 50 µM DEAB (C,D). Treatments were initiated during late blastula (st. 9.5), and by early gastrula (st. 10.25) the treatments were washed. RNA samples were collected at different time points during the recovery period. The response of RA target genes and genes encoding RA metabolic enzymes was studied by qPCR. Statistical significance (Student's t-test) was calculated compared to the expression level at the end of the treatment (t_0). *, $p<0.05$; **, $p<0.01$; ***, $p<0.001$; ****, $p<0.0001$; ns, not significant.

Figure 4. Retinoic acid signaling recovery in a kinetic analysis. (A) Schematic description of the experimental design to study the robustness of RA signaling and the transcriptomic changes involved in the maintenance of signaling robustness. **(B)** Principal Component Analysis of all six biological replicates revealed sample separation based on developmental stages. The samples grouped largely based on developmental time points following treatment, with the RA or DEAB groups clustering with the control samples. The t=0, 1.5, 3 and 4.5h

samples group were all distinctly separated by Principal Component 1. Principal Component 2 separated samples at intermediate time points (t=1.5 and 3h). The samples do not appear to separate based on experimental manipulation of RA levels for either PC1 or PC2. (C) Principal Component 8 revealed limited sample separation based on DEAB treatment (at t=3h) and RA addition (at t=1.5h). **(D)** Principal Component 10 revealed limited sample separation based on RA manipulation (t=1.5 and 3h). **(E)** Heatmap of gene expression of the top-100 positive and top-100 negative loadings corresponding to PC1, PC2, PC8 and PC10. A subset of the genes are highlighted based on their relevance to early developmental processes.

Figure 5. Comparison of the differential gene expression patterns across the two treatment groups compared to controls. (A) Genes were grouped into 27 discretized expression patterns based on three possible outcomes of expression (yellow: up-regulation, blue: down-regulation, grey: no change) at each of the three recovery time points compared to the t_0 sample. The numbers below each graph exemplify the discretized pattern as a numeric vector. For example, the pattern marked blue at only the last time point (first row) represents late down-regulation above a 2-fold change threshold. The counts next to the patterns indicate the number of genes that show the corresponding expression pattern in each of the two treatment groups and the controls. The pattern counts are based on a differential regulation threshold of 2-fold change compared to t=0. Only ten out of 27 dynamic patterns were exhibited by at least one gene and are included in the figure. The majority of genes showed differential regulation at 3 and 4.5h. Of note, no genes showed a biphasic response of up- and down-regulation within 4.5h. The progressive up-/down-regulation of genes constitute a dominant feature of the early developmental process, which in many instances represents a restoration of normal expression levels. **(B)** The Gene Ontology biological processes statistically enriched in the control group are indicated alongside the pattern counts. Details of statistical analysis results are available in Supplemental Table S1. **(C)** Venn diagrams to compare the overlap between the two treatments and control, illustrated for three differential gene expression patterns. The number of genes that show a similar differential expression pattern across two treatments and control is indicated in the middle of the Venn diagrams. The number of genes that showed similar differential expression patterns only in one or two experimental groups are also indicated in the corresponding overlapping regions of the Venn diagrams. Black, control; Orange, DEAB; Blue, RA.

Figure 6. Comparative pattern analysis to uncover the genes showing distinct changes in expression dynamics in response to opposing perturbations of the RA signal. (A) Genes were grouped into discretized expression patterns based on three possible outcomes of expression (yellow: up-regulation, blue: down-regulation, grey: no change) comparing either treatment versus control at each of the four recovery time points. For example, the pattern marked blue at all the time points (first column) represents persistent down-regulation. The two counts below the patterns indicate the number of genes that show the corresponding expression pattern in RA vs. control and DEAB vs. control. Only 32 out of 81 theoretically possible (four time points, 3*3*3*3=81) dynamic patterns were exhibited by at least one gene and are included in the figure. **(B)** COMPACT matrix comparing gene expression changes due to RA and DEAB relative to control. Of the potential 81x81 patterns, only the subset of 32 x 32 patterns with non-zero number of genes in either perturbation group are shown. The gene counts were grouped within related patterns based on the time of initial up- or down-regulation. Extended Data 1 contains a version of the COMPACT matrix shown with the gene identifiers corresponding to the counts. **(C)** Dynamic expression patterns of genes showing opposite changes in response to RA and DEAB treatments. This set of genes contains several components of the RA metabolism and gene regulatory network. **(D)** RA metabolic network showing synthesis and degradation of RA as well as a few known transcriptional regulatory targets. **(E)** Mapping the differential expression data onto the RA network shown in panel D to highlight the differences in regulation of biosynthesis versus degradation of RA signal between RA and DEAB groups.

Figure 7. Clutch-wise differential expression dynamics of select RA network genes and targets. The clutches are ordered left to right based on the earliest time at which *hoxa1* expression returned to the baseline levels. The data was combined from RNAseq (clutches A-F) and HT-qPCR (clutches G-L).

Figure 8. Trajectory analysis to compare the extent of multi-gene shift away from and return to control levels and rank clutch-wise robustness. (A) 3-dimensional principal curves for two separate gene sets: “RA pathway genes” and “HOX genes”, showing projections of the sample points on the curve. Black star indicates the beginning of the curve for the distance measurement along the path. **(B)** Principal curves with the projection of Control and treatment samples only for the clutch ranked “most shifted” or “least shifted”. Ranking of

clutches is based on the net (absolute) normalized shift of treatment samples from the corresponding Control sample for each time point. **(C,D)** A normalized expression shift profile calculated from the principal curve as the arc distance between the treatment and the corresponding control. Clutches are rank-ordered from lowest to highest net expression shift for HOX genes in the RA group. **(E,F)** Net (absolute) normalized shift of Hox genes (panel E) or RA metabolism genes (panel F) for each clutch over all time points, calculated for both RA and DEAB treatment. Clutches A-F data from RNA-seq , clutches G-L data from HT-qPCR.

Figure 9. Differential robustness to direction of change in RA level is related to the effectiveness of feedback regulatory action. (A) A schematic diagram of robustness efficiency matrix delineating the scenarios arising from all combinations of robustness and feedback response. **(B)** Distribution of clutches across the zones of the robustness efficiency matrix for RA and DEAB groups relative to the control. The letters indicate the distinct clutches. **(C,D)** Mapping the differential expression data onto the RA network shown in Fig. 6 to highlight the heterogeneity of differential regulation of RA network components amongst clutches closely situated in the robustness efficiency matrix (panel B). Clutches A,E, and F showed similar robustness efficiency in response to RA treatment (panel C), whereas clutches A, B, and D showed similar robustness efficiency in response to DEAB (panel D).

SUPPLEMENTAL INFORMATION:

Supplemental Figure S1. Genes affected by RA manipulation. Heatmap of gene expression of the top-100 positive and top-100 negative loadings corresponding to PC1, PC2, PC8 and PC10.

Supplemental Figure S2. Differential robustness to RA manipulation between embryo clutches. Principal Component Analysis of RNAseq data revealed heterogeneity across developmental stages and treatments. (A) Distribution of samples along PC1 and PC2 axes. (B) Distribution of samples along PC1 and PC10 axes. The letters represent the six distinct biological repeats, clutches A-F.

Supplemental Figure S3. HT-qPCR analysis of RA network components. Principal Component Analysis of HT-qPCR data revealed heterogeneity across developmental stages

and treatments. (A) Distribution of samples along PC1 and PC2 axes. (B) Distribution of samples along PC1 and PC10 axes. (C) Heatmap of time series differential expression of RA network genes.

Supplemental Figure S4. Clutch-wise heterogeneity in the response of RA network genes following RA manipulation. Clutch-wise differential expression dynamics of RA network genes. The clutches are ordered left to right according to the time taken for recovery of hoxa1.L.

Supplemental Figure S5. Trajectory analysis to compare the extent of multi-gene shift away from and return to control levels and rank clutch-wise robustness. Clutches are ordered left to right according to the extent of net deviation between control and RA treatment along the HOX gene trajectory. High deviation corresponds to low robustness and vice versa. (A) RA and control groups are highlighted along the trajectories. (B) DEAB and control groups are shown.

Supplemental Table S1. List of Gene Ontology annotations with corresponding genes and statistical significance corresponding to Figure 5.

Supplemental Table S2. Weighted Gene Correlation Network Analysis (WGCNA) of the time series RNAseq data. The green module is shown here.

Supplemental Table S3. List of HT-qPCR primers corresponding to the Hox genes and RA metabolic network.

Supplemental Table S4. RA network component polymorphisms between *Xenopus* strains. Based on Savova et al. (2017).

Extended Data 1. The Excel file contains the complete list of gene identifiers represented in the COMPACT matrix corresponding to Figure 6B.

Extended Data 2: The source Excel file contains all the gene expression modules from WGCNA.

Parihar et al.
Figure 1

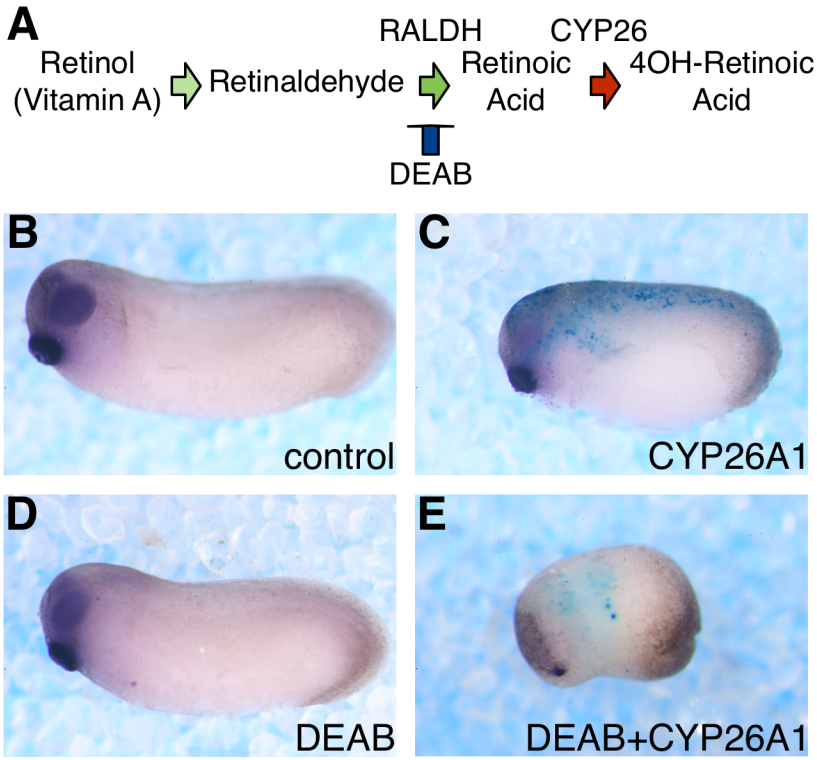

Parihar et al.
Figure 2

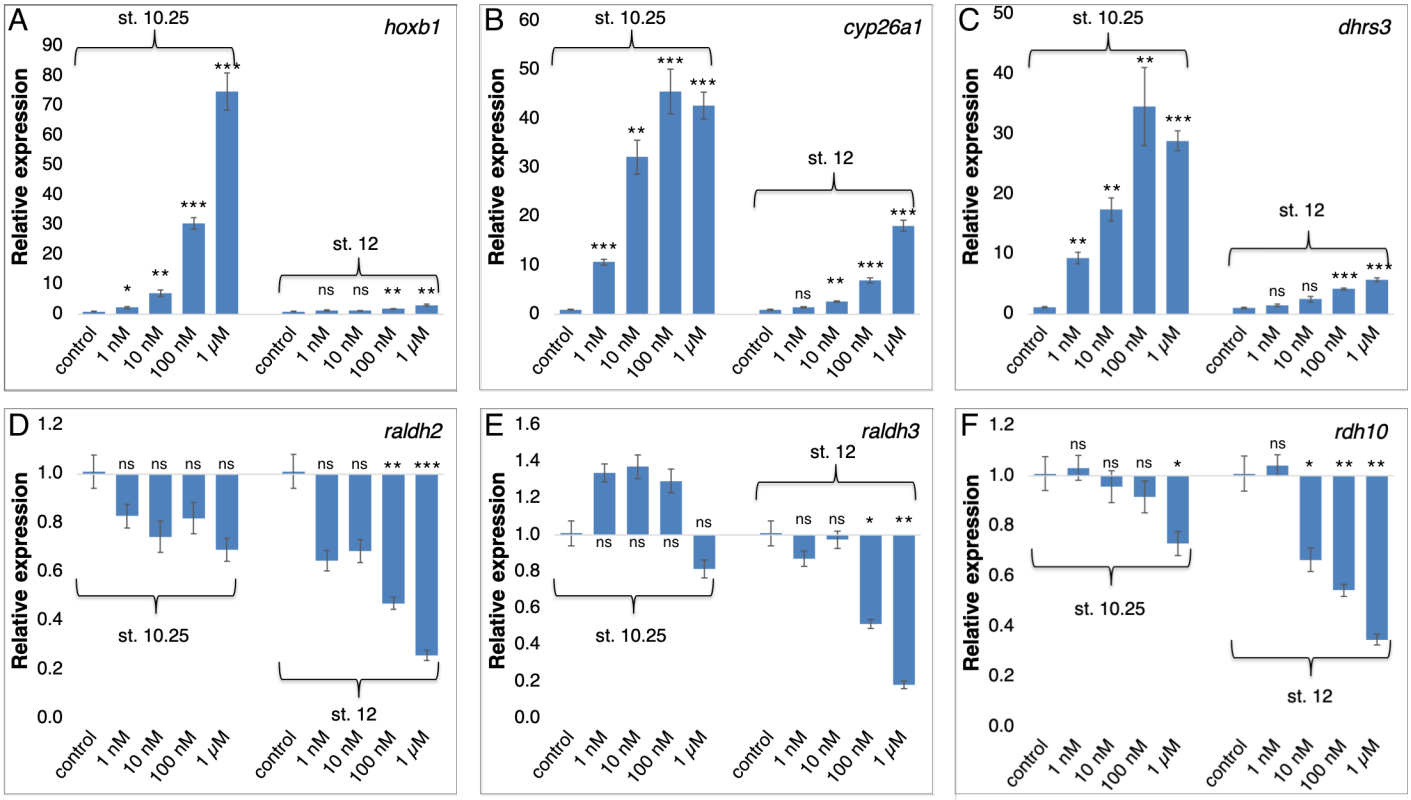

Parihar et al.
Figure 3

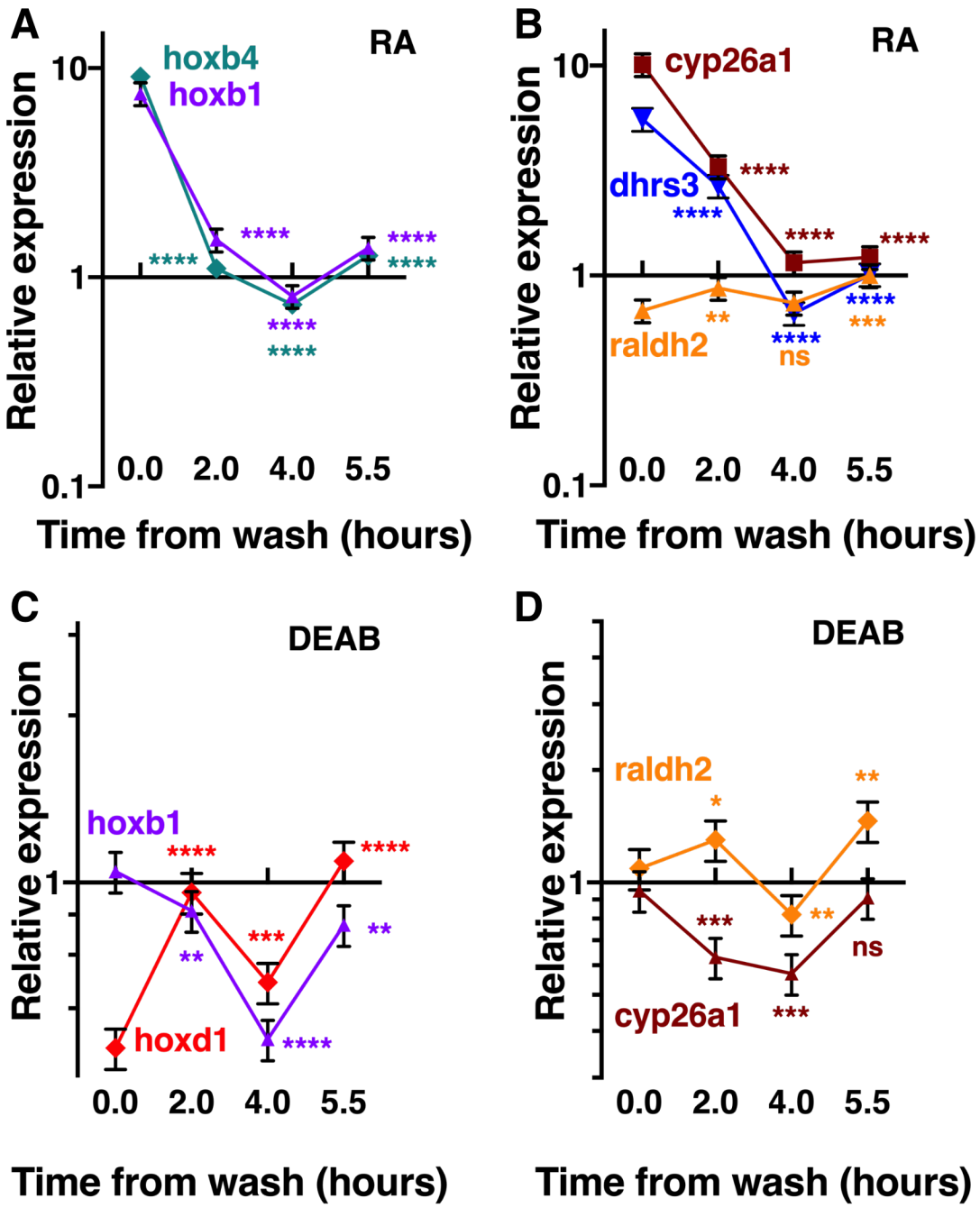

Parihar et al.
Figure 4

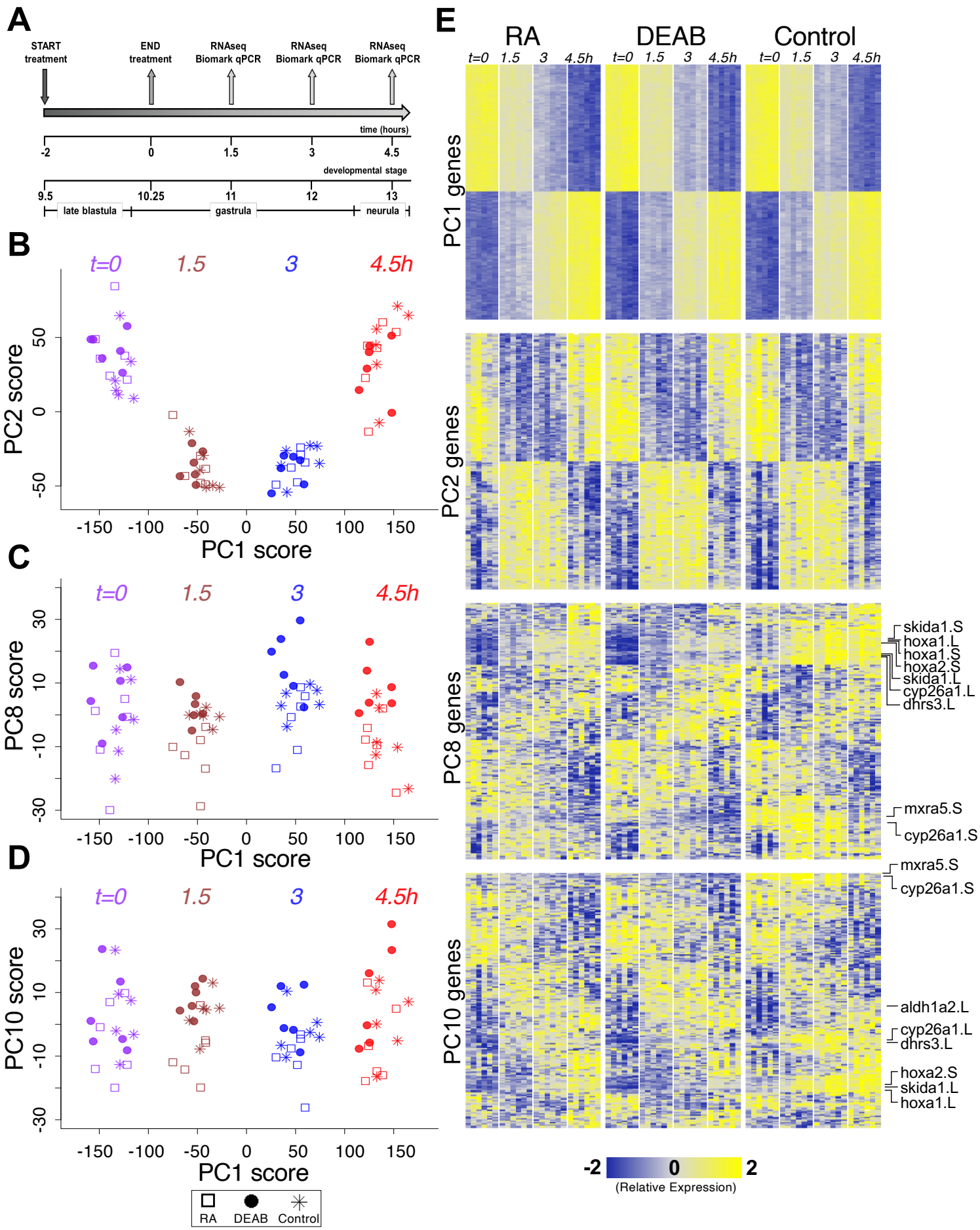

Parihar et al.
Figure 5

A

B

C

t = 0 1.5 3 4.5h	RA	DEAB	Control	Enriched Processes (Control Patterns)
0 0 0 -1	1074	1115	1175	regulation of insulin receptor signaling pathway / autophagy / fatty acid metabolic process / specification of symmetry
0 0 0 1	867	945	952	peptide metabolic process / cell fate specification / mesenchyme development / tissue migration
0 0 1 1	1013	975	937	animal organ development / cell adhesion / regulation of cell migration / positive regulation of cardiocyte differentiation
0 0 -1 -1	842	811	753	microtubule nucleation / positive regulation of signal transduction / endomembrane system organization
0 1 1 1	218	227	193	animal organ development / positive regulation of macromolecule biosynthetic process / Wnt signaling pathway / retinol metabolic process
0 -1 -1 -1	86	91	53	negative regulation of cell population proliferation / gastrulation
0 0 -1 0	58	38	37	regulation of cellular component organization / mitotic centrosome separation
0 0 1 0	23	27	18	myoblast differentiation
0 1 1 0	4	4	2	
0 -1 -1 0	1	1	1	

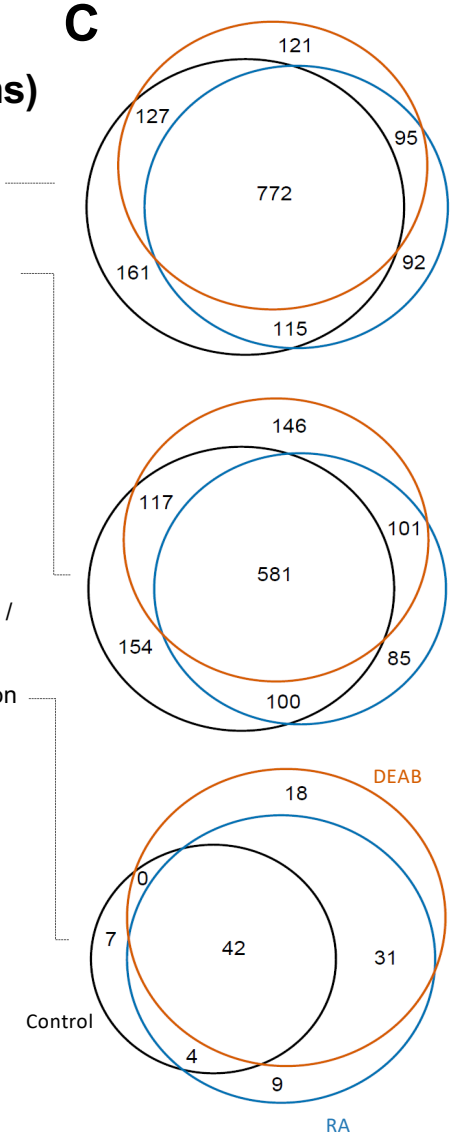

Parihar et al.
Figure 6

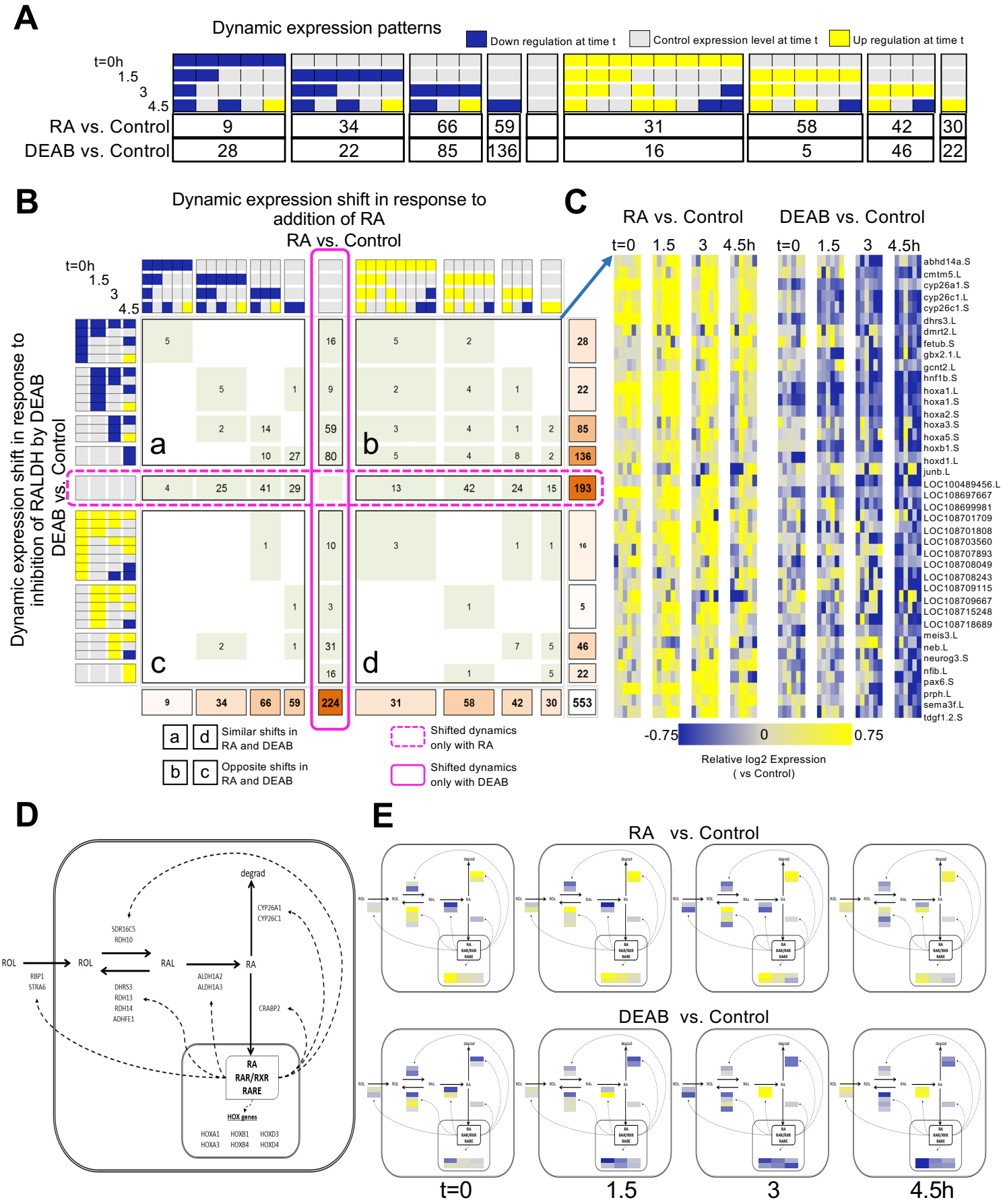

Parihar et al.
Figure 7

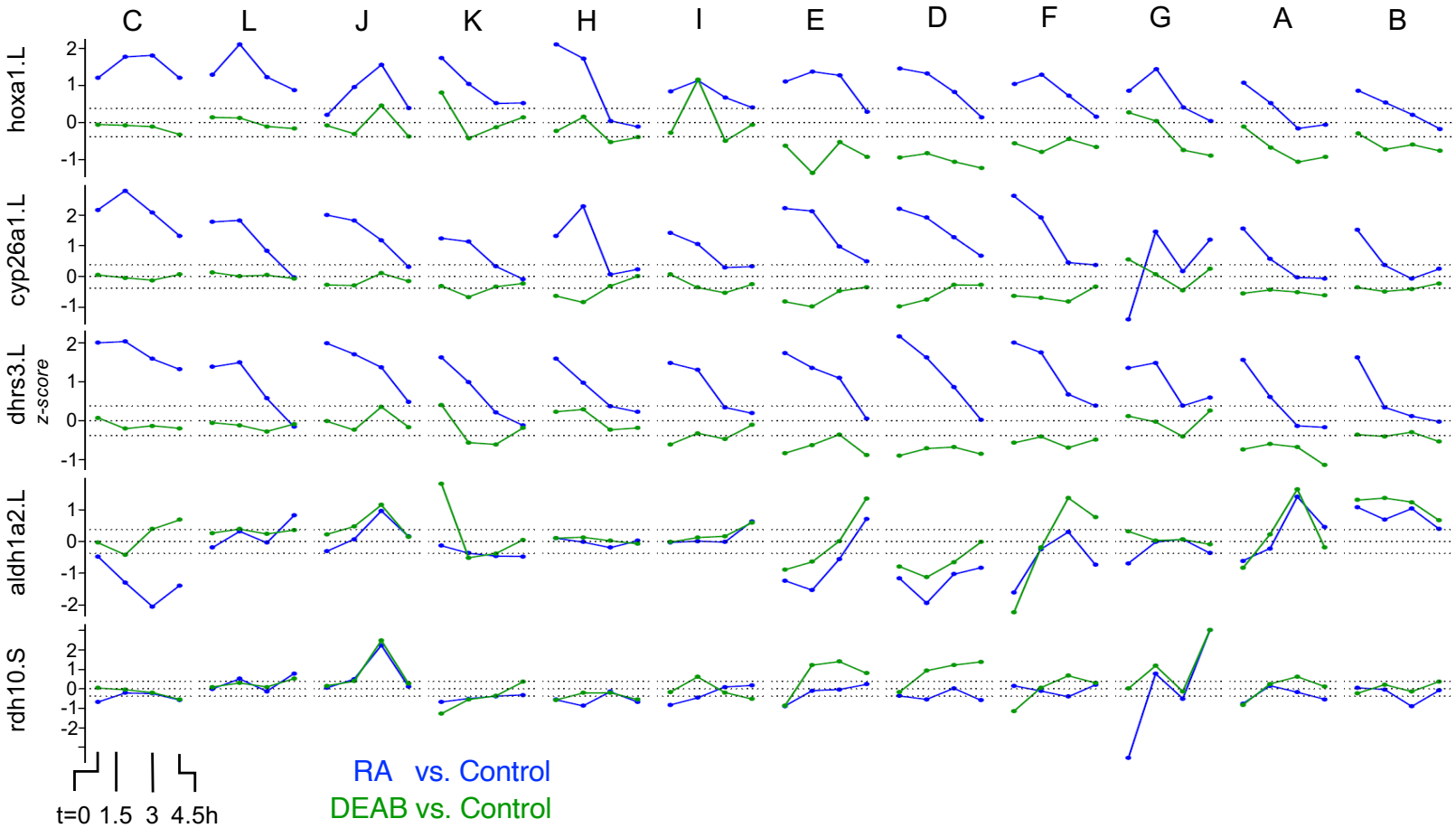

Parihar et al.
Figure 8

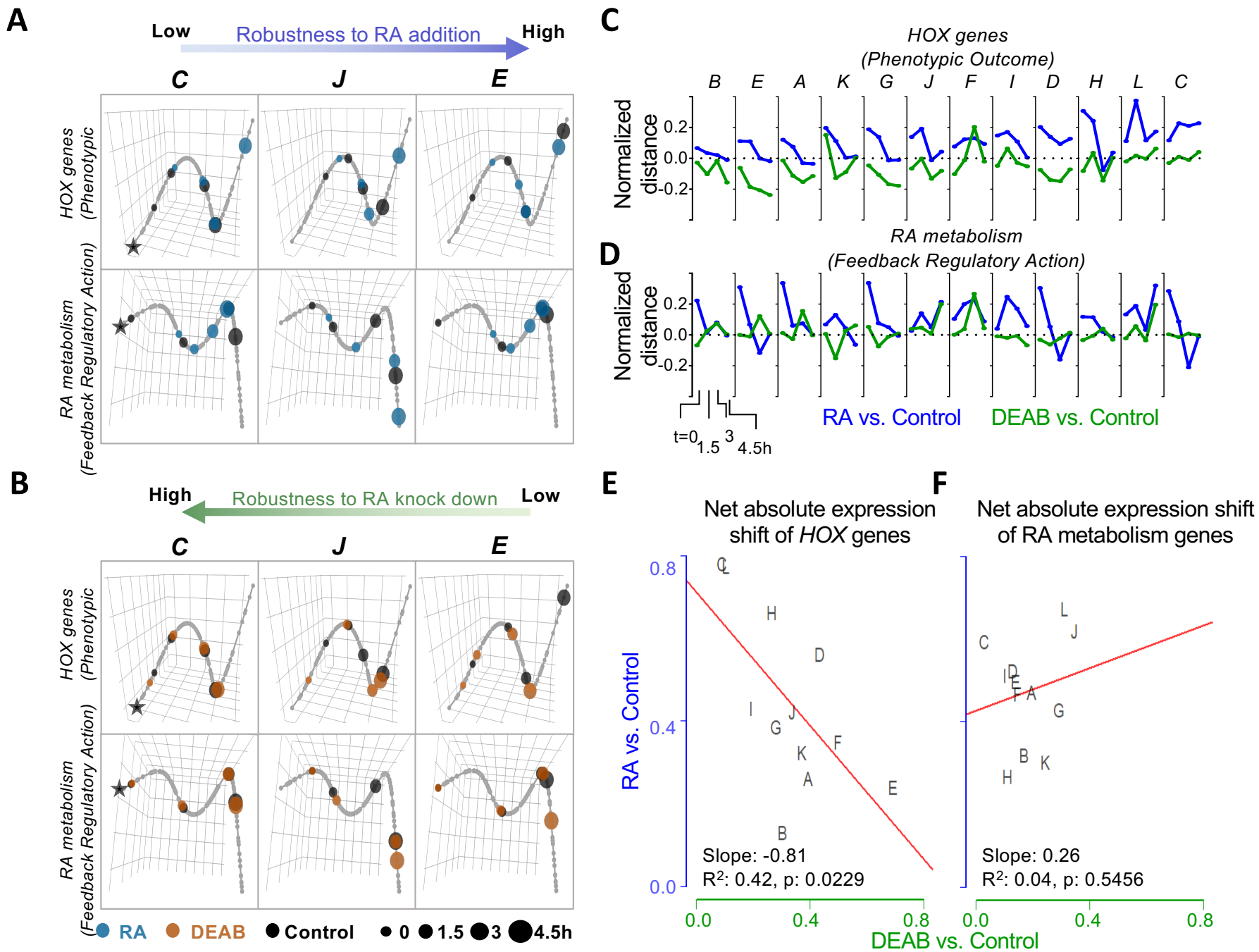

Parihar et al.
Figure 9

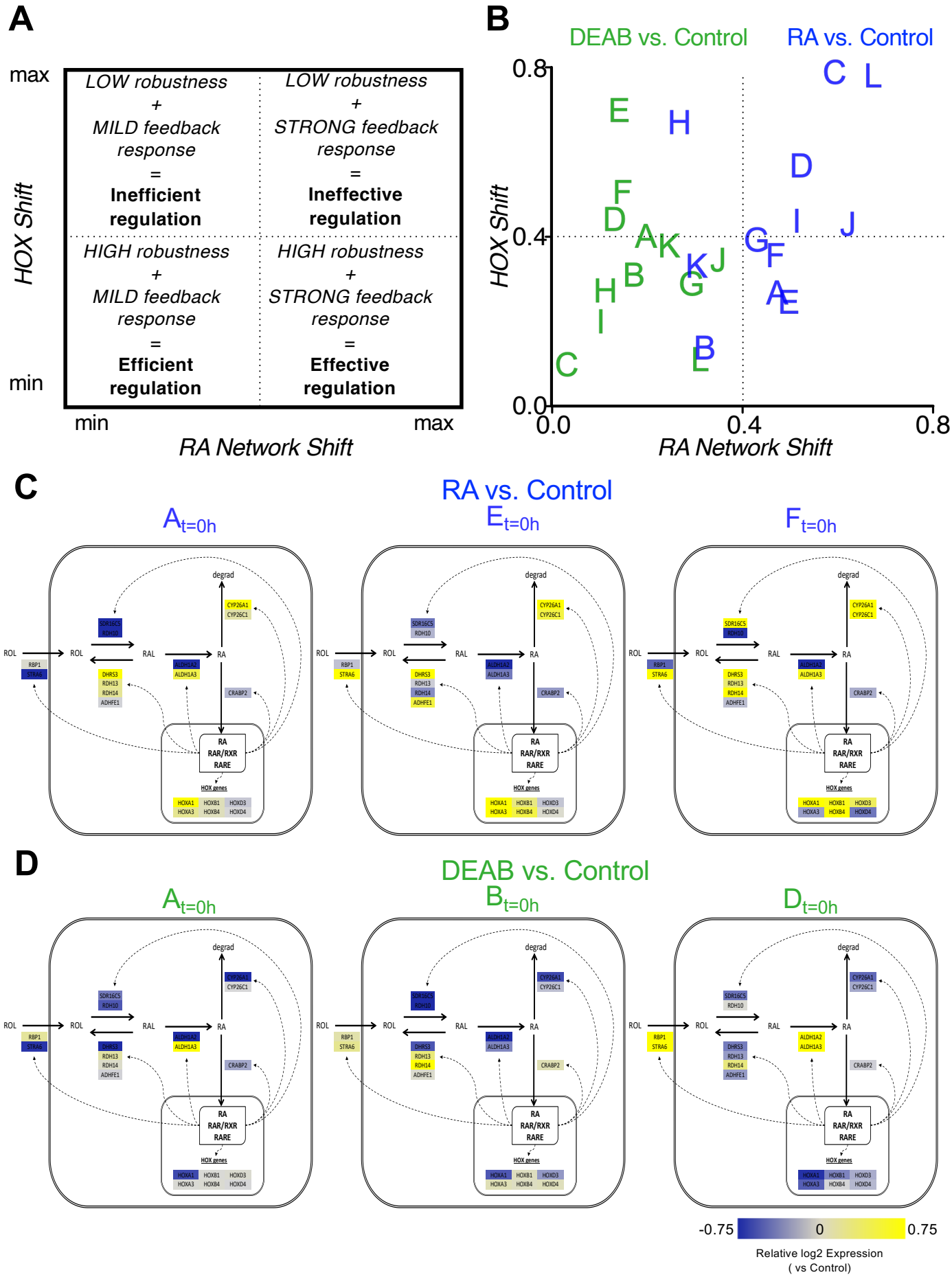

Parihar et al.
Supplemental Figure S1

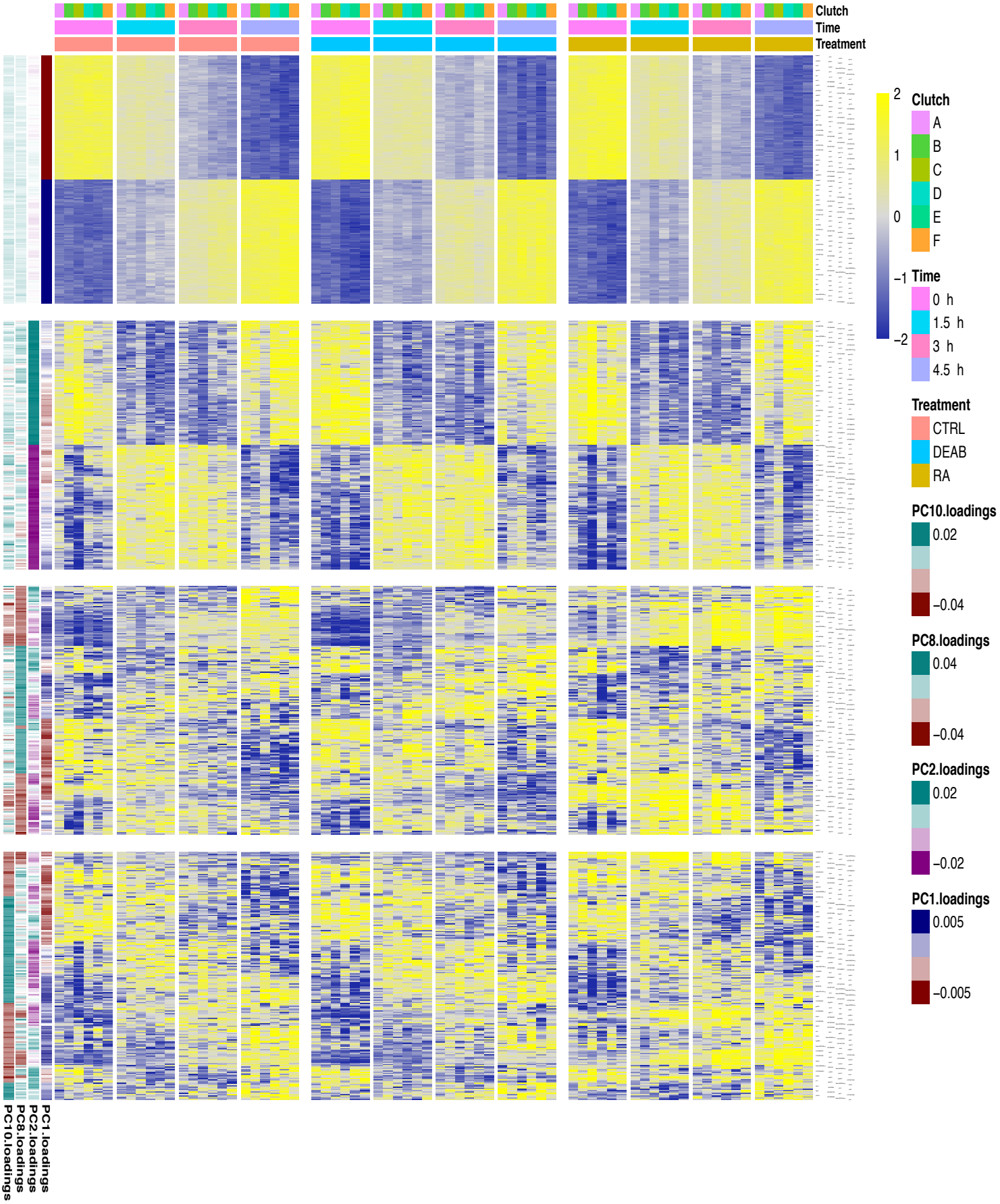

Parihar et al.
Supplemental Figure S2

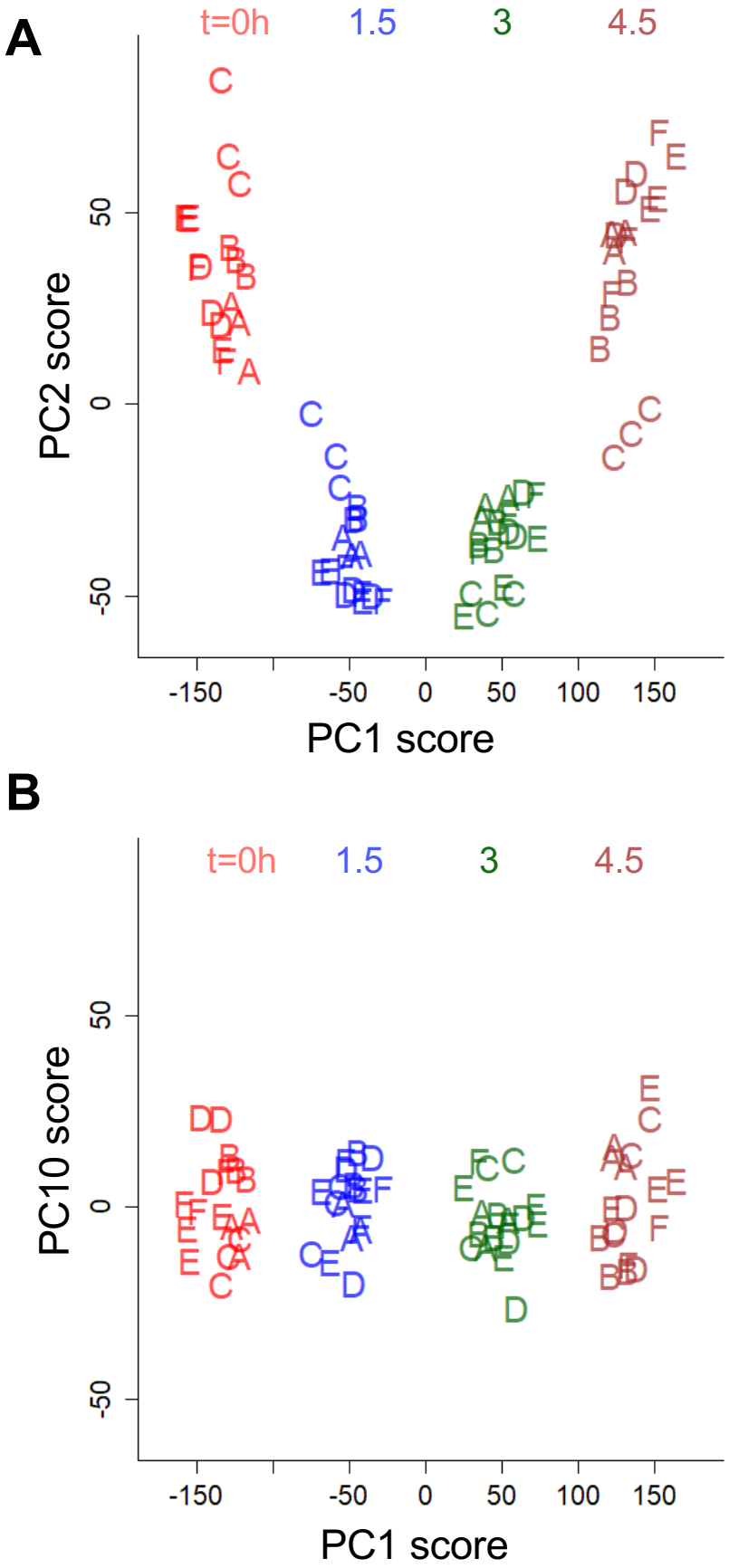

Parihar et al.
Supplemental Figure S3

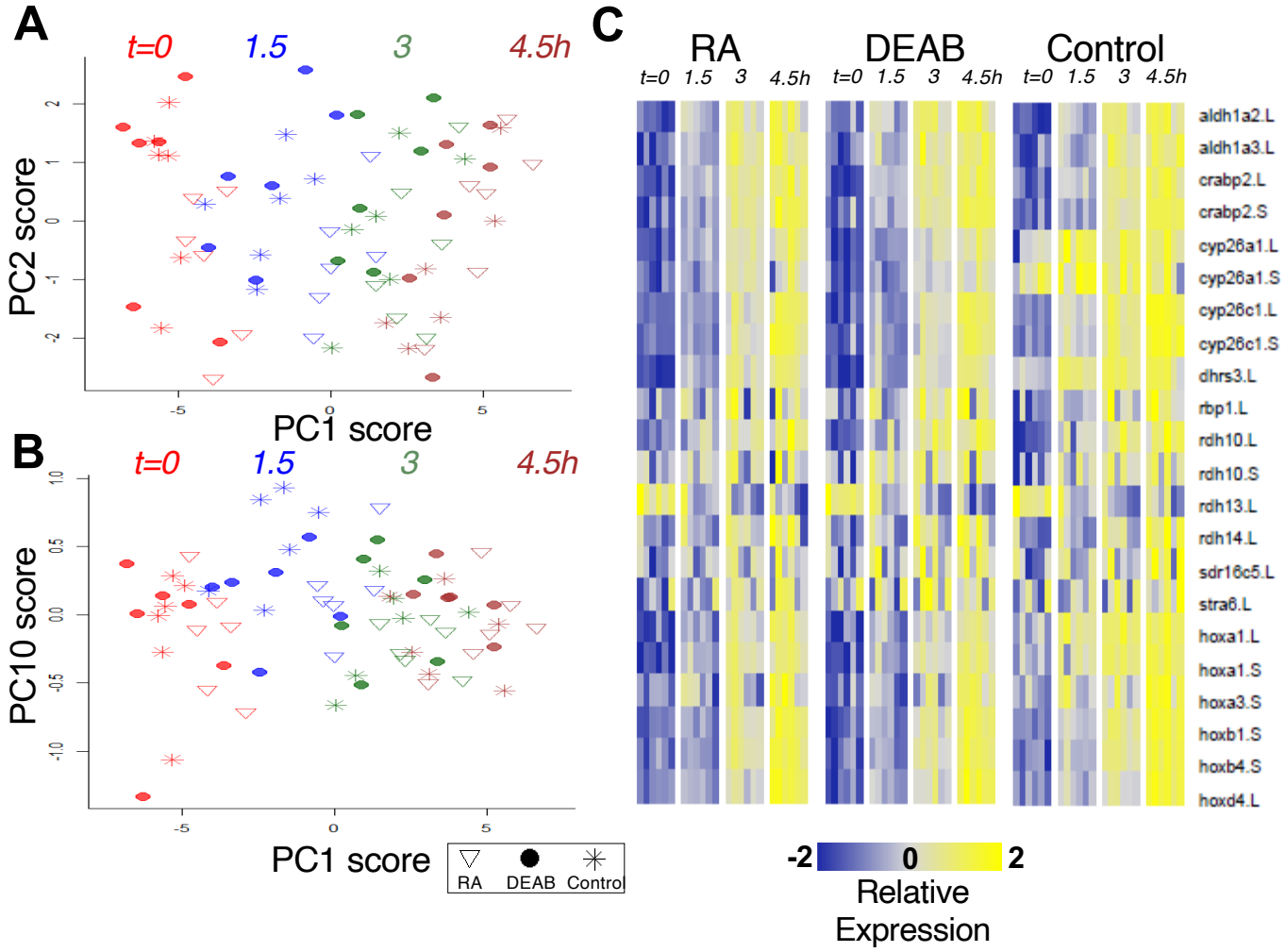

Parihar et al.
Supplemental Figure S4

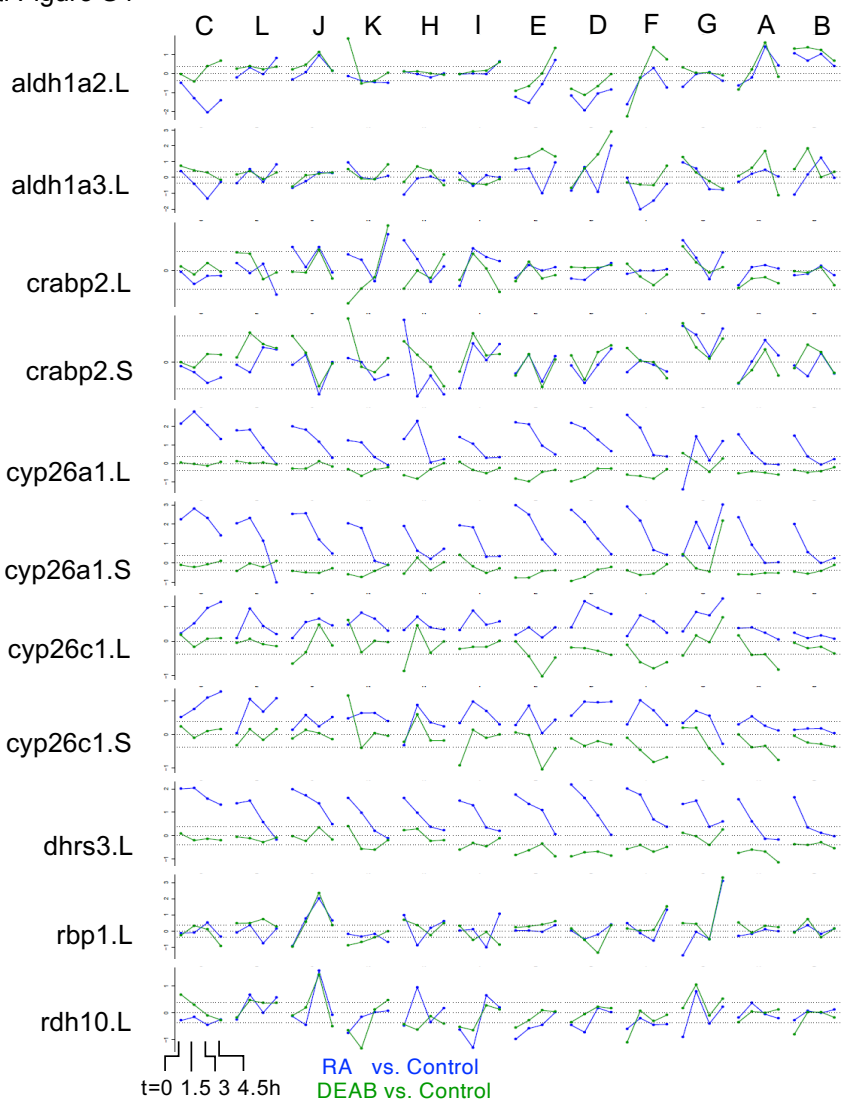

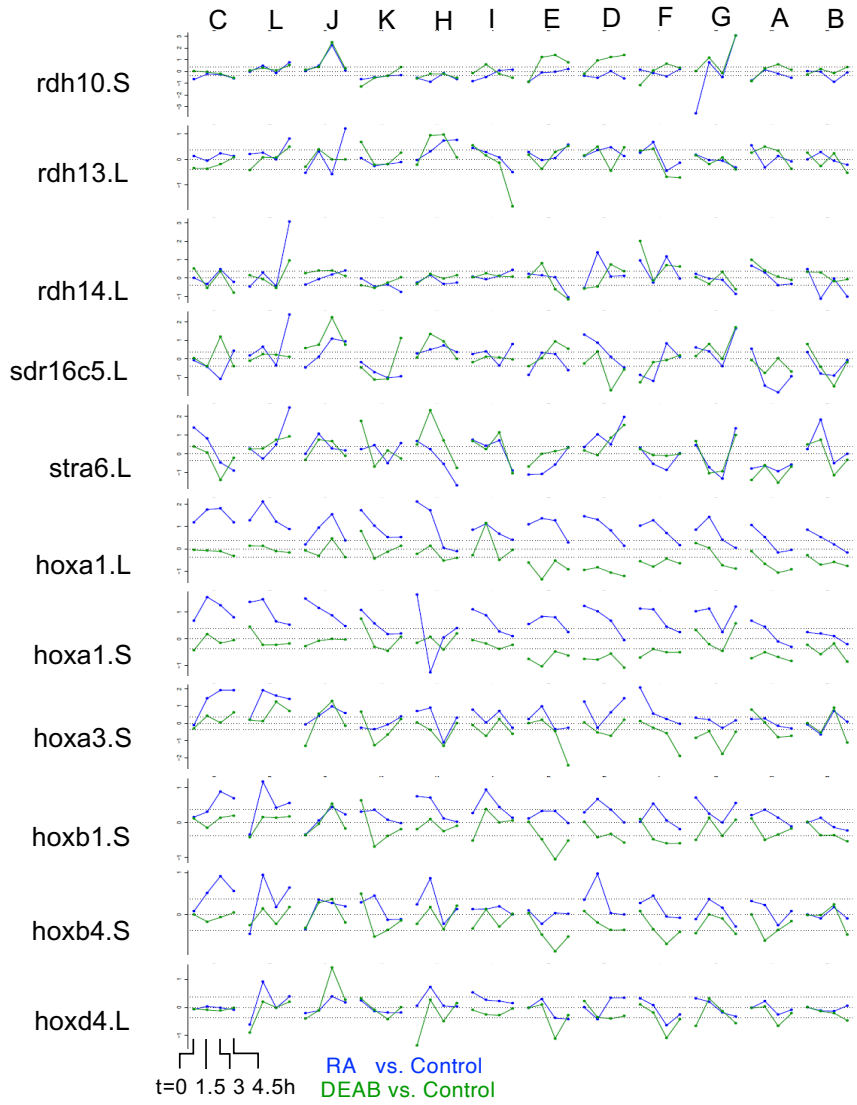

Parihar et al.
Supplemental Figure S5

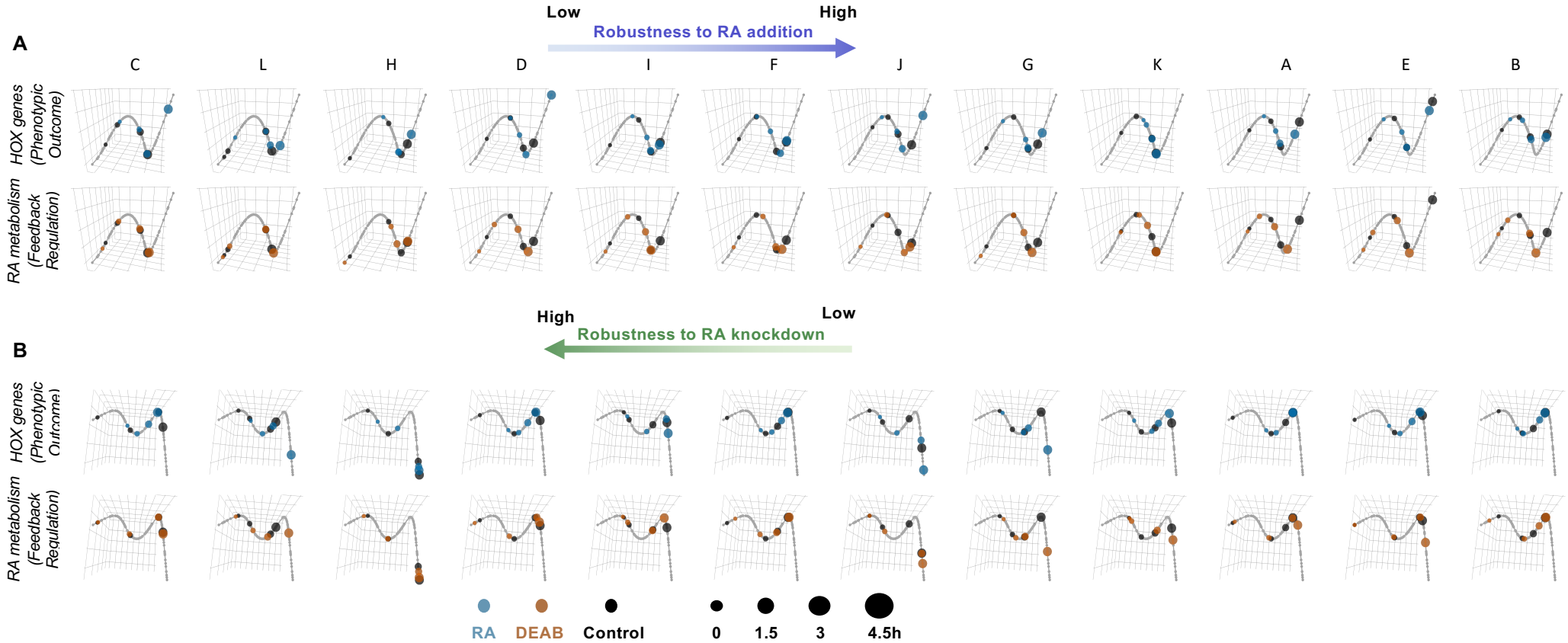

Supplemental Table S1. List of Gene Ontology annotations with corresponding genes and statistical significance corresponding to Figure 5.

Control Pattern	ID	Description	Total Genes	Pathway Genes	p value	adjusted q value
0 0 0 -1	GO:0046626	regulation of insulin receptor signaling pathway	426	5	2.90E-06	3.99E-03
	GO:0006914	autophagy	426	14	7.65E-05	1.50E-02
	GO:0006631	fatty acid metabolic process	426	11	1.45E-04	2.24E-02
	GO:0006096	glycolytic process	426	7	5.28E-04	3.80E-02
	GO:0008354	germ cell migration	426	3	7.55E-04	4.02E-02
	GO:0009799	specification of symmetry	426	5	1.04E-03	4.74E-02
	GO:0010876	lipid localization	426	13	1.07E-03	4.74E-02
0 0 0 1	GO:0006518	peptide metabolic process	302	44	5.82E-13	2.24E-10
	GO:0001708	cell fate specification	302	4	2.34E-03	2.11E-01
	GO:0060485	mesenchyme development	302	7	3.95E-03	2.68E-01
	GO:0090130	tissue migration	302	3	8.10E-03	4.42E-01
	GO:0010631	epithelial cell migration	302	2	8.83E-03	4.42E-01
0 0 1 1	GO:0048513	animal organ development	320	35	2.34E-08	1.95E-05
	GO:0007155	cell adhesion	320	26	3.21E-07	7.75E-05
	GO:0030334	regulation of cell migration	320	5	6.53E-03	7.35E-02
	GO:1905209	positive regulation of cardiocyte differentiation	320	2	9.88E-03	8.84E-02
0 0 -1 -1	GO:0007020	microtubule nucleation	250	3	3.01E-03	4.81E-01
	GO:0009967	positive regulation of signal transduction	250	9	5.54E-03	4.81E-01
	GO:0098927	vesicle-mediated transport between endosomal compartments	250	2	6.11E-03	4.81E-01
	GO:0010256	endomembrane system organization	250	7	6.13E-03	4.81E-01
0 1 1 1	GO:0048513	animal organ development	83	15	5.49E-07	1.25E-04
	GO:0048732	gland development	83	5	1.42E-06	1.25E-04
	GO:0010557	positive regulation of macromolecule biosynthetic process	83	11	3.29E-06	1.97E-04
	GO:0031328	positive regulation of cellular biosynthetic process	83	11	4.39E-06	1.97E-04
	GO:0016055	Wnt signaling pathway	83	8	2.71E-04	4.57E-03
	GO:0044344	cellular response to fibroblast growth factor stimulus	83	4	4.94E-04	6.21E-03
	GO:0010817	regulation of hormone levels	83	4	1.92E-03	1.84E-02
	GO:0042572	retinol metabolic process	83	2	2.43E-03	2.28E-02
0 -1 -1 -1	GO:0008285	negative regulation of cell population proliferation	15	3	7.57E-05	6.61E-03
	GO:0007369	gastrulation	15	2	5.21E-03	9.93E-02
0 0 -1 0	GO:0007100	mitotic centrosome separation	14	2	1.87E-05	2.16E-03
	GO:0140014	mitotic nuclear division	14	2	5.71E-03	8.00E-02
	GO:0051128	regulation of cellular component organization	14	3	8.47E-03	8.00E-02
	GO:0031338	regulation of vesicle fusion	14	1	8.51E-03	8.00E-02
	GO:0032418	lysosome localization	14	1	9.92E-03	8.00E-02
0 0 1 0	GO:0045663	positive regulation of myoblast differentiation	4	1	2.84E-03	1.71E-02
	GO:0045445	myoblast differentiation	4	1	3.25E-03	1.71E-02

Supplemental Table S2. Weighted Gene Correlation Network Analysis (WGCNA) of the time series RNAseq data. The green module is shown here. The attached Extended Data 2 source Excel file contains all the gene expression modules from WGCNA.

Gene ID	Gene Names	Module Numbers	Module Colors	RA vs. Control pattern	DEAB vs. Control pattern
Xelaev18001038	LOC108703560	5	green	1_1_1_1	0_0_-1_-1
Xelaev18002824	sema3f.L	5	green	0_0_1_1	0_0_0_-1
Xelaev18006802	nfib.L	5	green	0_0_1_1	0_0_0_-1
Xelaev18007035	cmtm5.L	5	green	1_1_1_0	0_0_-1_-1
Xelaev18010181	tdgf1.2.S	5	green	0_1_1_0	0_0_0_-1
Xelaev18012533	LOC108708243	5	green	0_0_0_1	0_0_0_-1
Xelaev18013332	prph.L	5	green	1_1_1_1	0_0_0_-1
Xelaev18014991	hnf1b.S	5	green	0_1_1_0	0_0_-1_-1
Xelaev18015206	LOC108709115	5	green	0_0_1_0	0_0_0_-1
Xelaev18024402	pax6.S	5	green	0_0_1_0	0_0_0_-1
Xelaev18024482	LOC108715248	5	green	0_1_1_0	0_0_0_-1
Xelaev18025805	abhd14a.S	5	green	0_1_0_0	0_0_-1_0
Xelaev18030578	LOC108718689	5	green	0_1_1_0	0_0_-1_-1
Xelaev18030982	hoxa1.L	5	green	1_1_1_0	-1_-1_-1_-1
Xelaev18031638	gcnt2.L	5	green	0_0_0_1	0_0_-1_0
Xelaev18033067	hoxa1.S	5	green	1_1_1_0	-1_-1_-1_-1
Xelaev18033068	hoxa2.S	5	green	1_1_0_0	0_-1_-1_-1
Xelaev18033069	hoxa3.S	5	green	1_0_0_0	0_0_0_-1
Xelaev18033072	hoxa5.S	5	green	0_0_1_0	0_0_0_-1
Xelaev18034595	cyp26c1.L	5	green	0_1_1_1	0_-1_-1_-1
Xelaev18035730	dhrs3.L	5	green	1_1_1_0	-1_0_0_-1
Xelaev18036884	cyp26a1.S	5	green	1_1_1_0	-1_-1_0_0
Xelaev18036885	cyp26c1.S	5	green	1_1_1_1	0_0_-1_-1
Xelaev18037155	neurog3.S	5	green	0_1_0_0	0_0_0_-1
Xelaev18037556	LOC108697667	5	green	1_1_1_0	0_-1_0_0
Xelaev18038437		5	green	0_0_1_0	0_0_0_-1
Xelaev18039368	meis3.L	5	green	0_1_0_0	-1_-1_0_0
Xelaev18041724	LOC108699981	5	green	0_1_1_0	0_0_-1_-1
Xelaev18044027	LOC108701808	5	green	0_1_1_0	0_-1_0_0
Xelaev18044028		5	green	1_1_1_0	0_0_0_-1
Xelaev18044734	hoxd1.L	5	green	0_1_0_0	-1_0_0_0
Xelaev18045501	LOC100489456.L	5	green	0_0_1_0	0_0_-1_-1
Xelaev18045983	hoxb1.S	5	green	0_1_0_0	0_-1_-1_-1
Xelaev18047280	gbx2.1.L	5	green	0_1_1_1	0_-1_-1_-1

Supplemental Table S3. List of PCR primers corresponding to the *hox* genes and RA metabolic network for RT-qPCR and HT-qPCR analysis.

Gene	*Forward primer*	*Reverse primer*
RT-qPCR		
dhrs3.L	CAGGCGCAAGAAATCCTAAG	CAAAGGCCACGTTACAGGAT
aldh1a2.L	ATGTTTGCCTGGAAGA	GAGAGCAGTGAGCGGA
cyp26a1.S	CGATTCCTCAAGGTTTGGCTTCA	ATTTAGCGGGTAGGTTGTCCACA
hoxb1.L	TTGCCCCAGTGCCAATGAC	TCCCCCTCCAACAACAAACC
hoxd1.S	TTCTTGCGGGGATGTTTTAG	CCGACTGGCATAAAGGAATG
hoxb4.S	CCAAGGATCTGTGCGTCAA	GCAGGATGGAGGCGAACT
gapdh	GCTCCTCTCGCAAAGGTCAT	GGGCCATCCACTGTCTTCTG
HT-qPCR		
aldh1a2.L	ATGTTTGCCTGGAAGATTGC	GAGAGCAGTGAGCGGAGTCT
cyp26c1.L	AAACGGGTTCCTTTCTGTGT	GCTTCGATTTACCCTACACTCTT
hoxb1.S	CCAACTTCACGACCAAACAA	GTGGCTGCGATCTCTACTCTC
hoxd4.L	TTCCCTACCATCATTCCTTTC	GAGTCATTATTTCCTGCTTTCTTT
rbp1.L	TGGAAATGCGAGTAGGAGATG	GGGATGGTGGTTTATTGTGTG
rdh13.L	CAAGTGTCTACCTGGCTGTTG	CCCAGAGTTTCCTTGCAGTT
rdh14.L	TGCCCGTACACAAAGACAGA	GAGACCAAGGAGGTGGTGAG
aldh1a3.L	TAAAGCCCTGTCTGTTTCT	CATACTCTCCAAGTTCCCTT
crabp2.L	AGCCACCCAAAGAAGACATAC	CGATAAGAAACGAAAGCAGAAA
crabp2.S	TCAAAGGAGATGGACCCAAGA	ATCAGCAGTCATGGTCAGGATAAG
cyp26a1.L	TCGAGGTTCGGCTTCATC	CGGCACAATTCCACAACA
cyp26a1.S	CCGCTTTCTAACGCCACTT	CACAATTCCACCACGAACAC
cyp26c1.S	AGCTCTGGTCCTTGAGATGG	AGCCAATGCAGAGTTTCTCC
dhrs3.L	CAGGCGCAAGAAATCCTAAG	CAAAGGCCACGTTACAGGAT
hoxa1.L	CCGCTCACTATATCCACCATTC	TGGCAGGAGAACGACAAAC
hoxa1.S	AATTATGAGATGATGGAATGGTAAA	TGACTGTAAACACCTAGTAAATGAGAG
hoxa3.S	AGCAGGGCAATGGAGTTT	GGAGGGTCCACCAGAATTAG
hoxb4.S	CCAAGGATCTGTGCGTCAA	GCAGGATGGAGGCGAACT
hoxd3.S	CTTCCCAGTCCACAATGAATAAA	GCTCTTCTCCTCGCAGTTCTC
rdh10.L	CGTCTCTTTGCCCTGGAGTTT	CACCATCTCCGCCGTCTC
rdh10.S	TTGCTTGGCCTGTAGAAGAGA	TGCATGGCGAAATAGGAGTAG
sdr16c5.L	TTTGTGGTTCCTTCCCTCTC	GTGCCATCAGTCTCCCTATACC
stra6.L	CCTGCTTACTTTCCTCCTGTTG	GTGGGTGACATTAAAGATTGTAGAGA
gapdh	GCTCCTCTCGCAAAGGTCAT	GGGCCATCCACTGTCTTCTG

Supplemental Table S4. RA network component polymorphisms between *Xenopus* strains[1]

Gene name	***Gene ID***	***aa position***	***aa1***	***aa2***
aldh1a2	18020673m	240	P	S
cyp26c1	18034595m	388	F	I
rbp1	18027898m	26	T	I
rbp1	18027898m	149	E	K
rbp1	18027898m	27	H	R
rdh10	18033799m	133	H	R
rdh13	18026677m	14	C	F
sdr16c5	18032037m	35	A	T
stra6	18018036m	610	S	N

[1]based on (Savova et al., 2017)